The Astrophysical Journal, 887:261 (19pp), 2019 December 20 https://doi.org/10.3847/1538-4357/ab5640

Exomoons in the Habitable Zones of M Dwarfs

Héctor Martínez-Rodríguez[1], José Antonio Caballero[2], Carlos Cifuentes[2], Anthony L. Piro[3], and Rory Barnes[4,5]
[1] Department of Physics and Astronomy and Pittsburgh Particle Physics, Astrophysics and Cosmology Center (PITT PACC), University of Pittsburgh, 3941 O'Hara Street, Pittsburgh, PA 15260, USA; hector.mr@pitt.edu
[2] Centro de Astrobiología (CSIC-INTA), ESAC, Camino Bajo del Castillo, E-28691 Villanueva de la Cañada, Madrid, Spain
[3] Carnegie Observatories, 813 Santa Barbara Street, Pasadena, CA 91101, USA
[4] Astronomy Department, University of Washington, Box 951580, Seattle, WA 98195, USA
[5] NASA Virtual Planetary Laboratory Lead Team, USA
Received 2019 June 1; revised 2019 October 26; accepted 2019 November 2; published 2019 December 26

Abstract

M dwarfs host most of the exoplanets in the local Milky Way. Some of these planets, ranging from sub-Earths to super-Jupiters, orbit in their stars' habitable zones (HZs), although many likely possess surface environments that preclude habitability. Moreover, exomoons around these planets could harbor life for long timescales and thus may also be targets for biosignature surveys. Here we investigate the potential habitability, stability, and detectability of exomoons around exoplanets orbiting M dwarfs. We first compile an updated list of known M-dwarf exoplanet hosts, comprising 109 stars and 205 planets. For each M dwarf, we compute and update precise luminosities with the Virtual Observatory spectral energy distribution Analyzer and *Gaia* DR2 parallaxes to determine inner and outer boundaries of their HZs. For each planet, we retrieve (or, when necessary, homogeneously estimate) their masses and radii, calculate the long-term dynamical stability of hypothetical moons, and identify those planets that can support habitable moons. We find that 33 exoplanet candidates are located in the HZs of their host stars and that four of them could host Moon- to Titan-mass exomoons for timescales longer than the Hubble time.

Unified Astronomy Thesaurus concepts: Astrobiology (74); Late-type dwarf stars (906); Dynamical evolution (421); Exoplanet systems (484)

Supporting material: machine-readable tables

1. Introduction

M dwarfs constitute only about one-third of the stellar mass of the Galaxy (Chabrier 2003), but about two-thirds of all its stars (Gould et al. 1996; Reid & Gizis 1997; Henry et al. 2006; Bochanski et al. 2010). Similar to their more massive stellar counterparts, M dwarfs also host exoplanets (Delfosse et al. 1998; Marcy et al. 1998; Butler et al. 2004; Bonfils et al. 2005, 2007, 2013a; Johnson et al. 2007; Udry et al. 2007; Dressing & Charbonneau 2015, among many others). Some of them orbit in the M-dwarf habitable zone (HZ), the circumstellar region where they can sustain liquid water on their surfaces (Hart 1979; Kasting et al. 1993; Scalo et al. 2007; Tarter et al. 2007; Ramírez 2018). The discoveries of such exoplanet candidates in temperate regions around their stars (e.g., Udry et al. 2007; Vogt et al. 2010, 2012; Anglada-Escudé et al. 2013, 2016; Tuomi et al. 2013; Dittmann et al. 2017; Gillon et al. 2017; Reiners et al. 2018) have come alongside theoretical calculations of HZs (Underwood et al. 2003; Selsis et al. 2007; Kopparapu et al. 2013; Zsom et al. 2013; Kopparapu et al. 2014; Barnes et al. 2015; Johns et al. 2018) and observational projects that aim to either discover Earth-like planets smaller than 1 $M_\oplus$ (e.g., Nutzman & Charbonneau 2008; Zechmeister et al. 2009; Bonfils et al. 2013a; Artigau et al. 2014; Quirrenbach et al. 2014; Ricker et al. 2015; Sullivan et al. 2015) or characterize their atmospheres (Wunderlich et al. 2019).

The M dwarfs' ubiquity and long main-sequence lifetime may favor their planets to host biological organisms (Segura et al. 2005; Loeb et al. 2016; Mullan & Bais 2018). However, given the low luminosities of M dwarfs (Delfosse et al. 2000; Reid & Hawley 2005; Benedict et al. 2016; Schweitzer et al. 2019), Earth-like planets in their HZs are located at short orbital separation to their stars, which enhances the probability to detect transits or induced radial velocity (RV) signals, translates into synchronous rotation, and consequently into tidal locking (Dole 1964; Peale 1977a, 1977b; Joshi et al. 1997; Murray & Dermott 1999; Tarter et al. 2007; Kite et al. 2011; Barnes 2017). This induced synchronous rotation has strong implications on the habitability of M-dwarf hosted planets because a hemisphere always faces the star and the other remains in complete darkness, introducing a spatially dependent incoming radiation and a temperature gradient between both hemispheres. Models of atmospheric circulation in dry, tidally locked, rocky exoplanets have shown that this circulation acts as a global engine that constrains large-scale wind speeds (Heng et al. 2011; Showman & Polvani 2011; Yang et al. 2013; Koll & Abbot 2016). Besides, in exoplanets that orbit close to their host stars, tidal interaction can affect climate stability, apart from spin and orbital properties (Kasting et al. 1993; Barnes et al. 2008; Heller et al. 2011a, 2011b; Shoji & Kurita 2014). In addition, flaring activity, which is frequent in M dwarfs (Jeffers et al. 2018; Loyd et al. 2018, and references therein), can cause strong atmospheric erosion in their exoplanets, with greater incidence on those that have no, or weak, magnetic moments (Buccino et al. 2006; Cnossen et al. 2007; Lammer et al. 2007; Segura et al. 2010; Vidotto et al. 2013; Shoji & Kurita 2014; France et al. 2018; Howard et al. 2018; Rodríguez et al. 2018). On the other hand, Driscoll & Barnes (2015) showed that core convection could still drive a strong geodynamo for gigayears on tidally locked worlds. Our knowledge of the atmospheres of Earth-like (and super-Earth) planets with one hemisphere under constant, strong irradiation is still incomplete, but the presence of a thick atmosphere or an ocean might help distribute the heat across

the planet (Joshi et al. 1997; Joshi 2003; Scalo et al. 2007; Tarter et al. 2007; Selsis et al. 2011; Heng & Kopparla 2012; Showman & Kaspi 2013; Kopparapu et al. 2014; Yang et al. 2014; Wordsworth 2015; Turbet et al. 2016; Way et al. 2018, see also Pierrehumbert & Gaidos 2011 for H_2-rich atmospheres).

One way to analyze the synchronous-rotation habitability problem of M-dwarf exoplanets is to introduce the presence of one or more hypothetical exomoons. Contrary to their host planets, exomoons would not become tidally locked to the star, but more likely to the planet itself (Hinkel & Kane 2013—see also Goldreich & Soter 1966 and Reynolds et al. 1987 for spin–orbit coupling of moons in our solar system). As a result, both exomoon hemispheres would receive the same amount of energy. The presence of an exomoon would also alleviate a second habitability problem: except for a few cases, the best characterized M-dwarf hosted exoplanets are super-Earths or mini-Neptunes with masses greater than 4–5 $M_\oplus$, which could be oceanic or gaseous worlds without any rocky surface, rather than Earth-like planets (Léger et al. 2004; Raymond et al. 2004; Lammer et al. 2009; Hill et al. 2018). In this picture, exomoons of about the mass of the Earth (with masses large enough to have a carbon–silicate cycle) would be habitable in the anthropocentric view, as opposed to their more massive planet hosts.

Exomoons could also have effects on the habitability of their host exoplanets. For instance, the Moon contributes to steady the Earth's obliquity, which might have allowed life to develop in stable conditions for a sufficiently long time (Laskar et al. 1993, 2004; Lourens et al. 2001; although see Armstrong et al. 2014; Deitrick et al. 2018). It is considered that moons are more stable and have longer lifetimes when the planet/moon systems are further from the parent star, the planets are heavier, or the parent stars are lighter (Barnes & O'Brien 2002; Sasaki et al. 2012; Sasaki & Barnes 2014). In addition to the flux received by the host star, a moon's climate and, thus, its habitability, can also be affected by planetary insolation and thermal emission, by periodic stellar eclipses, and by tidal heating (Zollinger et al. 2017). Tidal interactions between exoplanet and exomoon are a source of heating that is more relevant for the latter, such as in the inner Galilean moons (Yoder 1979; Peters & Turner 2013; Makarov & Efroimsky 2014; Clausen & Tilgner 2015; Tyler et al. 2015; Renaud & Henning 2018). Moderate tidal heating may help sustain tectonic activity, possibly a carbon–silicate cycle, and may also provide energy for biochemical reactions (Campanella 2009; Kaltenegger 2010; Heller 2012; Heller & Barnes 2013; Hinkel & Kane 2013; Heller et al. 2014; Forgan & Dobos 2016; Zollinger et al. 2017).

Exomoons are yet to be discovered (Kipping et al. 2013, 2015—but see the three *Kepler* candidates reported by Szabó et al. 2013, and especially Kepler-1625 b—Teachey et al. 2018; Teachey & Kipping 2018; Heller et al. 2019; Kreidberg et al. 2019). Most planet detection techniques are not applicable to that of exomoons due to the small relative sizes in comparison with their host planets. One of the most relevant techniques is the transits method, but it relies upon favorable geometric conditions and high photometric precision (Kipping et al. 2009, 2012). For the majority of exoplanet–exomoon phase curves, the lunar component is undetectable to the current technology of transits observations, and future surveys would require a photometric precision of a few parts per million (Forgan 2017, but see again Teachey & Kipping 2018). Nevertheless, the detectability of exomoons has been proposed feasible with current or near-future technology and a variety of methods: microlensing (Han & Han 2002), photocentric transit timing variation (Simon et al. 2007, 2015), modulation of planetary radio emissions (Noyola et al. 2014), spectroastrometry (Agol et al. 2015), polarization of transits (Berzosa Molina et al. 2018), radial velocity (Vanderburg et al. 2018), and transits of the plasma torus produced by a satellite (Ben-Jaffel & Ballester 2014; see the reviews by Cabrera & Schneider 2007; Perryman 2018, and Heller 2018). In particular, the European Space Agency (ESA) mission *CHaracterising ExOPlanet Satellite* (*CHEOPS*) could detect Earth-sized exomoons with the transit method (Simon et al. 2015).

Here, we explore the potential habitability of exomoons around known M-dwarf exoplanets. We compile a state-of-the-art list of M-dwarf exoplanetary systems, derive precise stellar luminosities from multiwavelength photometry and *Gaia* DR2 parallaxes, apply conservatively the radiative transfer equilibrium equation, identify exoplanets in HZ that can be orbited by exomoons, discuss their detectability, and investigate their long-term dynamical stability based on the latest models by Piro (2018), who modeled exoplanets torqued by the combined tides of an exomoon and a host star in order to find timescales for the gravitational loss/destruction of the exomoon.

2. Analysis

2.1. Stellar and Exoplanet Sample

As of 2019 March 19, the Extrasolar Planets Encyclopaedia[6] had reported a total of 4011 exoplanets with the label "confirmed" (Schneider et al. 2011). In our analysis, first, we discarded the 258 planets detected by direct imaging (123), microlensing (88), pulsar timing (33), transit timing variation (8), and astrometry (6), many of which are located at large distances from the solar system and orbital separations, suffer from strong high-energy radiation, are difficult to characterize, or even are bona fide brown dwarfs (Caballero 2018).

Of the remaining 3734 planets, 205 orbit 109 systems with M-dwarf hosts detected via transit and/or radial velocity. To identify them, we selected all planets orbiting stars with M spectral type in the Extrasolar Planets Encyclopaedia except for nine giants and subgiants (HD 208527, HD 220074), pre-main-sequence stars (CVSO 30, V830 Tau), and spectroscopic, eclipsing, and close binaries (DW UMa, HD 41004 B, Kepler-64, KIC 5095269 AB, NLTT 41135). Besides, we selected all planets orbiting stars without spectral type in the Encyclopaedia, but with masses lower than 0.71 $M_\odot$, which is the largest mass of an M dwarf in the Encyclopaedia, and that have M spectral type in the NASA Exoplanet Archive.[7] Among the 205 exoplanets, we also included the planets orbiting the trio of stars BD–21 784, BD–06 1339, and Kepler-155 (Lo Curto et al. 2013; Rowe et al. 2014; Tuomi et al. 2014), which have been spectroscopically classified as stars at the K–M boundary (Upgren et al. 1972; Stephenson 1986; Zechmeister et al. 2009; Muirhead et al. 2012a; Gaidos et al. 2013; Tuomi et al. 2014), and LP 834-042 c, which is listed in the Encyclopaedia as `detection_type=Other` but has a radial velocity confirmation (Astudillo-Defru et al. 2017b).

[6] http://exoplanet.eu/
[7] https://exoplanetarchive.ipac.caltech.edu/

Table 1
Exoplanets with True Masses and Radii

Star	Planet	Transit References[a]	RV References[a]
HATS-6	b	Har15	Har15
PM J11302+0735	b	Clo17	Sar18
Kepler 45	b	Jon12	Jon12
LHS 1140	b	Dit17	Dit17
	c	Men19	Men19
LHS 3275	b	Har13	Cha09
LP 424–4	b	Bon12	Bon12
LTT 3758	b	Sou17	Bon18
PM J11293-0127	b	Sin16	Alm15
	c	Sin16	Alm15
	d	Sin16	Alm15
Ross 905	b	Mac14	Tri18
USco J161014.7-191909	b	Man16b	Man16b

Note.
[a] Alm15: Almenara et al. (2015); Bon12: Bonfils et al. (2012); Bon18b: Bonfils et al. (2018a); Cha09: Charbonneau et al. (2009); Clo17: Cloutier et al. (2017); Dit17: Dittmann et al. (2017); Har13: Harpsœet al. (2013); Har15: Hartman et al. (2015); Jon12: Johnson et al. (2012); Mac14: Maciejewski et al. (2014); Man16b: Mann et al. (2016b); Men19: Ment et al. (2019); Sar18: Sarkis et al. (2018); Sin16: Sinukoff et al. (2016); Sou17: Southworth et al. (2017); Tri18: Trifonov et al. (2018).

The 109 M dwarfs and 205 exoplanets are listed in the Appendix tables. For the stars, we tabulate common/discovery and alternative names,[8] equatorial coordinates and parallactic distances from *Gaia* DR2 (Gaia Collaboration et al. 2018), except for Luyten's star and Lalande 21185, for which we used *Hipparcos* parallactic distances (van Leeuwen 2007). Distances range from merely 1.30 pc (Proxima Centauri; Anglada-Escudé et al. 2016) to about 430 pc (Kepler-235; Borucki et al. 2011). All stars further than 30 pc have been discovered by *Kepler* (and *K2*) except for NGTS–1 and HATS–6 (Hartman et al. 2015; Bayliss et al. 2018). Besides, most of them are field M dwarfs, but at least four belong to stellar cluster members or associations (namely K2-25 in the Hyades–Mann et al. 2016a, K2-33 in Upper Scorpius–Mann et al. 2016b, K2-95 and K2-264 in the Praesepe–Pepper et al. 2017; Livingston et al. 2019).

For the planets, we tabulate their names, letters, main orbital parameters (semimajor axes a and orbital periods $P_{\rm orb}$), and corresponding references. For the 43 planets without a published semimajor axis (e.g., Rowe et al. 2014; Muirhead et al. 2015; Sahlmann et al. 2016), we derived them from their known periods and our estimated stellar masses, using *Kepler*'s Third Law. For the 89 planets discovered with the RV method and without measured transits, we tabulate their minimum masses, $M_2 \sin i$ (marked with ">"), while for the 103 planets discovered with the transit method and without RV follow-up, we tabulate their radii. We have true masses and radii for 13 transiting planets with RV follow-up in 10 systems (see Table 1).

[8] We follow this naming priority order: common (e.g., Proxima, Luyten's star), Bayer (e.g., α Cen C), Flamsteed/variable (e.g., 3 Lyr, IL Aqr, V1428 Aql), Lalande, Henry Draper, Bonner/Córdoba Durchmusterung, Wolf, Ross, Gliese-Jahreiss (but GJ number is always given), Luyten Palomar or equivalent, and discovery names (e.g., MCC, PM, 2MUCD, *Kepler*, *K2*, KOI, EPIC).

2.2. Planetary Masses and Radii

RV measurements only yield the minimum mass of an exoplanet, whereas transit measurements only yield the radius. For our habitability analysis, we used planet masses and radii. However, only 13 planets have both RV and transit measurements, i.e., true masses and radii (see above). As a result, for the other 192 planets, we derived planetary radii and masses. Among the multiple mass–radius relations available in the literature for different planetary compositions (e.g., Fortney et al. 2007; Seager et al. 2007; Sotin et al. 2007; Lissauer et al. 2011; Barnes et al. 2013; Wu & Lithwick 2013; Weiss & Marcy 2014; Barnes et al. 2015; Rogers 2015; Wolfgang et al. 2016; Chen & Kipping 2017; Kanodia et al. 2019), we chose that of Chen & Kipping (2017), as it covers a broad range of planetary sizes.

The largest planet transiting an M dwarf is NGTS–1 b, with $R \sim 1.33\,R_{\rm Jup}$ (Bayliss et al. 2018). On the other side of the relation, the smallest planets transit the stars Kepler 138 b, LSPM J1928+4437 (b, c, and d), Kepler-125 c, and 2MUCD 12171 (now universally known as TRAPPIST-1; d and h), and have masses and radii in the intervals 0.10–0.39 $M_\oplus$ and 0.52–0.78 $R_\oplus$, close to the values of Mars (0.107 $M_\oplus$, 0.343 $R_\oplus$). However, the distributions of masses and radii of the whole planet sample peak around 5–10 $M_\oplus$ and 1–3 $R_\oplus$, respectively.

2.3. Stellar Luminosities and Masses

First of all, we compiled *Gaia* DR2 equatorial coordinates (in J2015.5 epoch and J2000.0 equinox) with VizieR (Ochsenbein et al. 2000) for 107 of our stars. For the other two, Lalande 21185 and Luyten's star, without a *Gaia* DR2 entry, we retrieved the equatorial coordinates from Two Micron All Sky Survey (2MASS; Skrutskie et al. 2006), which were separated by less than two months from the J2000 epoch. Next, we collected multiband broadband photometry from the ultraviolet to the mid-infrared from the literature: *GALEX* DR5 (FUV, NUV; Bianchi et al. 2011), SDSS DR9 (*ugri*; Ahn et al. 2012), UCAC4 (*BV*, *gri*; Zacharias et al. 2013), Pan-STARRS1 DR1 (*gri*; Tonry et al. 2012; Chambers et al. 2016), Tycho-2 (B_T, V_T; Høg et al. 2000) APASS9 (*BV*, *gri*; Henden et al. 2016), 2MASS (*JHK*$_s$; Skrutskie et al. 2006), *Gaia* DR2 ($G_{BP}\,G\,G_{RP}$; Gaia Collaboration et al. 2016, 2018), *WISE* (*W*1*W*2*W*3*W*4; Cutri et al. 2012), and allWISE (*W*1*W*2*W*3*W*4; Cutri et al. 2014).

For that, we used the Upload X-Match tool of the interactive graphical viewer and editor for tabular data TOPCAT (Ochsenbein et al. 2000) with a search radius of 5″ and the "Best" find mode option. We made sure that the automatic cross-match was right by carrying out an inspection of each individual target and datum using the Aladin interactive sky atlas (Bonnarel et al. 2000), which provides simultaneous access to digitized images of the sky, astronomical catalogs, and databases. Eventually, for the 109 stars we compiled 1682 individual magnitudes along with their uncertainties.

We homogeneously derived the bolometric luminosity and effective temperature for each star with the compiled photometric data and the Virtual Observatory Spectral Energy Distribution Analyzer[9] (VOSA; Bayo et al. 2008). We selected the best fit between a grid of BT-Settl-CIFIST theoretical

[9] http://svo2.cab.inta-csic.es/theory/vosa/

spectral models (Baraffe et al. 2015) and our empirical data under the constraints $\log g = 4.5$, $2000\,\mathrm{K} < T_{\mathrm{eff}} < 4500\,\mathrm{K}$, and $[\mathrm{Fe/H}] = 0.0$. The VOSA fits are acceptable in all cases, except for the extremely young star K2-33 in the Upper Scorpius association (David et al. 2016; Mann et al. 2016b; Schweitzer et al. 2019) and the metal-poor star K2-155 (Díez Alonso et al. 2018b; Hirano et al. 2018). Further details on the luminosity calculation will be described by C. Cifuentes et al. (2019, in preparation).

The luminosities of the 109 planet-host stars are displayed in the Appendix. As expected, the most luminous stars are at the K–M boundary, with $L \sim 0.14$–$0.17\,L_{\odot}$. In particular, the most luminous stars, Kepler-155 and Kepler-252, have VOSA-derived $T_{\mathrm{eff}} = 4300$–$4400\,\mathrm{K}$, which are actually warmer than the hottest known M dwarfs (thus, their spectral types should be revised). On the other side, the least luminous stars, with $L = (5\text{–}15) \times 10^{-4}\,L_{\odot}$, are the latest and coolest ones, which in our case are 2MUCD 12171 and Proxima Centauri, which have M8.0 V and M5.5 V spectral types, respectively.

Finally, we computed stellar masses from K_s magnitude and distance using the relations of Mann et al. (2019). We display them in the last column of Table 5. The lowest masses, $M_* = 0.09$–$0.12\,M_{\odot}$, are found again for 2MUCD 12171 and Proxima Centauri, and the highest ones, $M_* = 0.67$–$0.70\,M_{\odot}$, correspond to the likely late-K dwarfs Kepler-155 and Kepler-252, K2-33 (actually incorrect, due to its extreme youth), and K2-155 (probably due to a metallicity effect). For comparison, we compiled published luminosities for 26 stars from the following works: Leggett et al. (2001), Howard et al. (2010), Boyajian et al. (2012), Gaidos & Mann (2014), Quintana et al. (2014), Hartman et al. (2015), Schlieder et al. (2016), Dittmann et al. (2017), Gillon et al. (2017), Maldonado et al. (2017), Bakos et al. (2018), Hirano et al. (2018), Ribas et al. (2018), Smith et al. (2018), Affer et al. (2019), Díez Alonso et al. (2019), Feinstein et al. (2019), Günther et al. (2019), Hobson et al. (2019), and Perger et al. (2019). The luminosities derived in this work are in good agreement with the values given in the literature (see Figure 1). Only five stars deviate more than 20% of the 1:1 ratio, but only one deviates significantly from our measurement. For BD–17 400, we calculated $L = (835 \pm 13) \times 10^{-4}\,L_{\odot}$, but Leggett et al. (2001) tabulated $L = (450 \pm 70) \times 10^{-4}\,L_{\odot}$ with pre-*Gaia* data. The other four stars have luminosities consistent within error bars with our measurements (LP 656–38,[10] Leggett et al. 2001; GJ 96, Gaidos & Mann 2014; Kepler-186, Quintana et al. 2014; K2-149, Hirano et al. 2018).

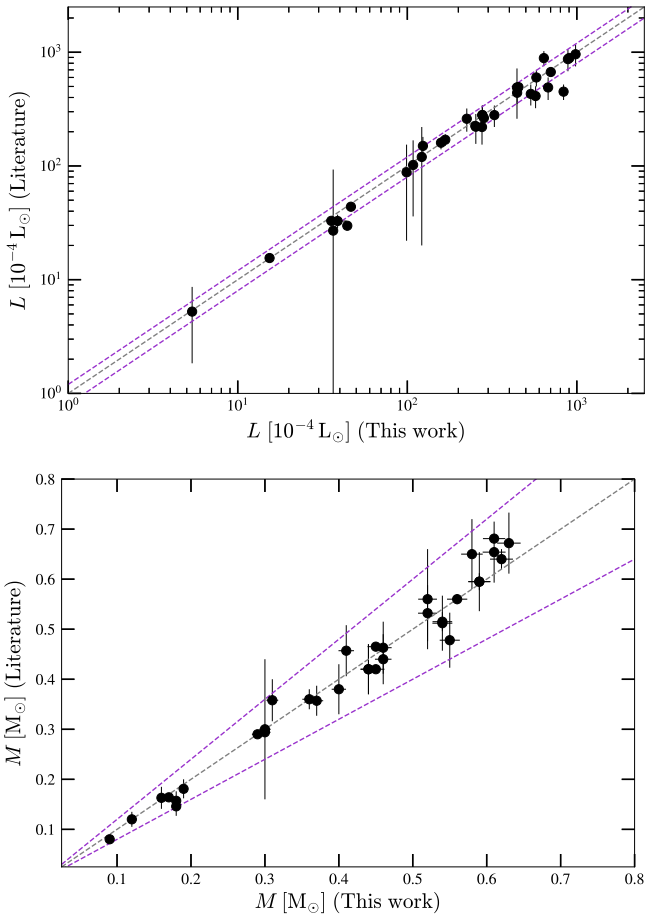

Figure 1. Comparison between our luminosities (top) and masses (bottom) and those available in the literature. The dashed lines indicate the 1:1 ratio and 20% variations with respect to it.

3. Results and Discussion

3.1. Exoplanet Habitability

We calculated an HZ for each host star using the one-dimensional climate models from Kopparapu et al. (2014). We chose their "recent Venus" and "maximum greenhouse" estimates for the inner and outer HZ, respectively. The exoplanets' oceans might begin to evaporate and condense in the stratosphere at planetary equilibrium temperatures ≈320–340 K ("moist–greenhouse," Kasting et al. 1993; Kopparapu et al. 2013, 2014). However, between this process and the complete oceanic evaporation (runaway greenhouse limit, Kasting et al. 1993; Kopparapu et al. 2013, 2014), the exoplanets could still have surface temperatures adequate for habitability ("continuosly HZ," Hart 1978; Kasting et al. 1993).

Figure 2 illustrates the HZ computation for our compiled exoplanet-host M dwarfs. The exoplanet candidates are depicted in three different colors, depending on whether they lie between their host stars and the inner HZ boundary (146), whether they lie between the inner and outer HZ boundary (33), or whether they lie beyond the outer HZ boundary (26). The 33 potentially habitable exoplanets are marked with the string "Yes" in column "Potentially HZ" from Table 6. Of the 33 planet candidates, 10 have masses or minimum masses above $10\,M_{\oplus}$ and 9 between 5 and $10\,M_{\oplus}$. Not counting the inclination angle effect in the RV planets, which translates into larger actual masses, most if not all of these 19 planets are mini-Neptunes and can hardly sustain liquid water on a rocky surface (Fortney et al. 2007; Miller-Ricci et al. 2009; Dorn et al. 2017). In other words, these 19 planets lie within the HZ of their stars, but they are unlikely to be habitable. However, their Earth-sized moons could actually be habitable.

As illustrated by Figure 2, three habitable planets are beyond the approximate 1 Gyr-tidal locking boundary: BD–06 1339 c (Lo Curto et al. 2013), Kepler-186 f (Torres et al. 2015), and HD 147379 b (Reiners et al. 2018). Of them, two are Neptune-like planets and one, Kepler-186 f, has a mass of only about $1.8\,M_{\oplus}$. However, following Barnes (2017), they will likely be tidally locked after 4.6 Gyr, the solar system age (see

[10] Leggett et al. (2001) tabulated $L = (27 \pm 66)10^{-4}\,L_{\odot}$ for LP 656–38.

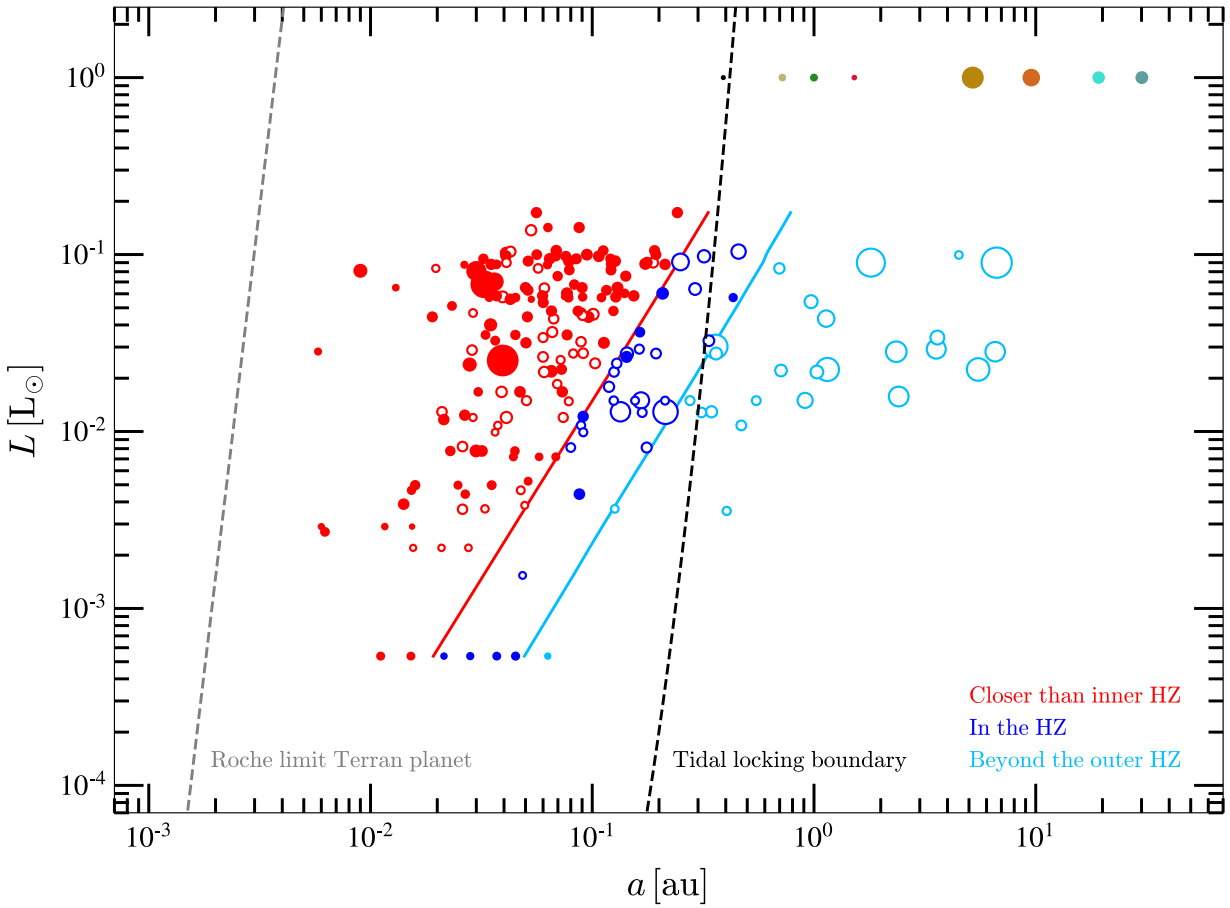

Figure 2. Conservative HZ for all the M dwarfs in our sample (inner HZ, "recent Venus," in red; outer HZ, "maximum greenhouse," in sky blue). Their hosted exoplanets are depicted with sizes proportional to their masses in logarithmic scale, with filled circles if they have been detected by transit and with open circles if they have been detected by RV measurements. Exoplanets closer than the inner HZ, in the HZ, and beyond the outer HZ are shown in red, neon blue, and sky blue, respectively. The dashed, gray line is the Roche limit for an Earth-like planet (Aggarwal & Oberbeck 1974). The dashed, black line represents a "constant-time-lag" tidal locking model for a 10 $M_\oplus$-planet with rapid initial rotation after 1 Gyr (Barnes 2017). The eight solar system planets are depicted in the upper part of the plot.

Section 3.2 for an individualized computation of planet locking times).

3.2. Exomoons around Potentially Habitable Exoplanets

We focused on the 33 exoplanets orbiting the HZ of their host stars and analyzed whether or not they could host exomoons on reasonable timescales. For that, we followed the work of Piro (2018), who considered null exomoon eccentricity and obliquity for simplicity. If an exoplanet hosting an exomoon is close enough to its host star, the star's gravity strips the exomoon away. This critical distance, namely the radius of the Hill sphere, is given by:

$$a_{\mathrm{crit},m} = f_{\mathrm{crit}} \left(\frac{M_{\mathrm{p}}}{3M_*} \right)^{1/3}, \quad (1)$$

where M_{p} and M_* are the exoplanet and star masses, and $f_{\mathrm{crit}} = 0.49$, a critical factor that assumes a prograde orbit (Domingos et al. 2006; Piro 2018). Eventually, the exomoon will be stripped away by the host star if $a_m > a_{\mathrm{crit},m}$, or fall back into the planet if $a_m < a_{\mathrm{crit},m}$, where a_m is the moon semimajor axis around the exoplanet.

If an exomoon gets too close to its host exoplanet, it will be tidally disrupted upon reaching the Roche limit, i.e., the point where the exomoon can no longer bind its material by gravitational forces. This condition is given by (Piro 2018):

$$a_{\mathrm{Roche}} \approx 1.34 \left(\frac{M_{\mathrm{p}}}{\rho_m} \right)^{1/3}, \quad (2)$$

where ρ_m is the exomoon's density (see also Aggarwal & Oberbeck 1974). Under the assumption that all the initial angular momentum of an exoplanet eventually goes into its exomoon, the exomoon's semimajor axis can be written as:

$$a_m = \frac{4\pi^2 \lambda^2 M_{\mathrm{p}} R_{\mathrm{p}}^4}{G M_m^2 P_0^2}, \quad (3)$$

where λ ($\lambda_\oplus = 0.33$, Williams 1994) is the exoplanet's radius of gyration ($I_{\mathrm{p}}/M_{\mathrm{p}}R_{\mathrm{p}}^2$, see Piro 2018), M_m is the exomoon mass, I_{p} is the planet moment of inertia, R_{p} is the planet radius, and P_0 is the planet initial spin period. To estimate the exomoon migration timescale, namely, the e-folding timescale for the change in the exoplanet–exomoon distance, we used Equation (25) from Piro (2018), which can be rewritten as:

$$\tau_{\mathrm{mig},m} = t_k \left(\frac{k_{2,\oplus}}{k_2} \right) \left(\frac{\tau_{\mathrm{lag},\oplus}}{\tau_{\mathrm{lag}}} \right) \left(\frac{a_m^8}{M_m R_{\mathrm{p}}^5} \right), \quad (4)$$

where $t_k = 250$ Gyr, and a_m, M_m, and R_{p} are the exoplanet–exomoon separation, exomoon mass, and planetary radius in

units of Earth–Moon separation, Moon mass, and Earth radius, respectively.[11] Here, k_2 is a Love number of degree 2 ($k_{2,\oplus} = 0.3$) and $\tau_{\rm lag}$ is the time lag between the passage of the perturber and the tidal bulge (Barnes 2017; Green et al. 2017; Piro 2018). For the Earth, $\tau_{\rm lag,\oplus} = 638$ s (Lambeck 1977; Neron de Surgy & Laskar 1997). The time lag $\tau_{\rm lag}$ is related with the tidal quality factor Q via (Henning et al. 2009; Matsumura et al. 2010; Barnes et al. 2013):

$$Q^{-1} \approx n\tau_{\rm lag}, \tag{5}$$

where n is the mean motion, which implies that

$$\frac{\tau_{\rm lag,\oplus}}{\tau_{\rm lag}} = \frac{Q}{Q_\oplus}, \tag{6}$$

where $Q_\oplus = 12$ (Williams et al. 1978). Therefore, combining Equations (3), (4) and (6),

$$\tau_{{\rm mig},m} \propto Q\frac{R_{\rm p}^{27}M_{\rm p}^{8}}{P_0^{16}M_m^{17}}. \tag{7}$$

Table 2 summarizes the used values of k_2, Q, and λ for four representative planetary types. These parameters are reasonable extrapolations of k_2, Q, and λ from models of exoplanets and actual measurements of planets of different sizes and compositions (Dickey et al. 1994; Yoder 1995; Aksnes & Franklin 2001; Zhang & Hamilton 2006; Henning et al. 2009). For planets with sizes between $R_{\rm p} = 1.50\,R_\oplus$ (small, rocky worlds) and $R_{\rm p} = 3.88\,R_\oplus$ (Neptune), we fitted a linear function to k_2:

$$k_2 = k_{2,0} + \gamma\,R_{\rm p}. \tag{8}$$

For Q and λ, we fitted, respectively, two power laws and two linear functions, between $R_{\rm p} = 1.50\,R_\oplus$ and $R_{\rm p} = 3.88\,R_\oplus$, and between $R_{\rm p} = 3.88\,R_\oplus$ and $R_{\rm p} = 10.97\,R_\oplus$ (Jupiter):

$$Q = Q_0\,R_{\rm p}{}^{\delta} \tag{9}$$

and

$$\lambda = \lambda_0 + \epsilon\,R_{\rm p}. \tag{10}$$

The values resulting from these fittings are listed in Table 3. Next, we computed the parameters $a_{\rm Roche}$, a_m, and $\tau_{{\rm mig},m}$ for the 33 exoplanets in HZ with a hypothetical exomoon. In our calculations, we set $M_m = M_{\rm Moon}$ and $\rho_m = 2500\,{\rm kg\,m^{-3}}$, which is a density intermediate between those of Io and Ganymede, but slightly lower than that of the Moon (that has a small iron core formed after the collision between Theia and the proto-Earth). The Roche limit, $a_{\rm Roche}$, smoothly depends on ρ_m (Equation (2)). For example, assuming the Earth density $\rho_\oplus = 5513\,{\rm kg\,m^{-3}}$, $a_{\rm Roche}$ would only be increased by 23%. Next, we set $a_m = a_{{\rm crit},m}$ in Equation (4) when the exomoon is stripped ($a_m > a_{{\rm crit},m}$) and used the value given by Equation (3) when it falls back ($a_m < a_{{\rm crit},m}$). We did not calculate $\tau_{{\rm mig},m}$ if $a_m < a_{\rm Roche}$. We remark that, for multiplanetary systems, these estimates may not be entirely accurate because of the impact of the other planets.

The initial planetary spin P_0 is one of the greatest unknowns in such estimates. It is the orbital period, as opposed to the initial rotation period, which would be set by the last major impact. Figure 3 shows the orbital periods for all the exoplanets in our sample. Minimum and maximum $P_{\rm orb}$ range from 4.3 hr (K2-137 b; Smith et al. 2018) to 24 yr (BD–05 5715 c; Montet et al. 2014), but they concentrate between 1 and 50 days. The range of $P_{\rm orb}$ for the exoplanets in HZ is narrower, from 4 to 130 days, with a median value of 31 days. For completeness, the median $P_{\rm orb}$ for inner and outer HZ planets are 7 days and 502 days, respectively.

Figure 4 depicts $a_{{\rm crit},m}$ versus $a_{\rm Roche}$ for the 33 potentially habitable planets in our sample. It shows the two most extreme cases: $P_{0,1} = P_{\rm orb}$ and $P_{0,2} = 3.0$ hr. On the one hand, $P_{0,1} = P_{\rm orb}$ ($\tau_{{\rm mig},m} \propto Q\,R_{\rm p}^{27}M_{\rm p}^{8}P_0^{-16}$) is the longest allowed value of P_0 because the exoplanet is tidally locked to its star. It is probably the most realistic case, as the habitable exoplanets in our sample orbit their stars under synchronous rotation. In particular, we computed the tidal locking time $t_{\rm lock}$ with "constant-phase lag" (CPL, where the phase between the perturber and the tidal bulge is constant and insensitive to orbital and rotational frequencies) and "constant-time lag" (CTL, where the time interval between the perturber's passage and the tidal bulge is constant) models, using the publicly available `EqTide`[12] code and the Proxima Centauri b system as a template (Barnes et al. 2016; Barnes 2017). We assumed zero eccentricity and obliquity, an initial planetary spin period of 3.0 h, a stellar Love number $k_{2,*} = 1.5$, a stellar gyration radius $\lambda_* = 0.1$ ($\lambda_\odot = 0.061$, Bouvier 2013), and the planetary parameters k_2, Q, λ varying accordingly with $R_{\rm p}$. We chose the minimum $t_{\rm lock}$ between the calculations from the CPL and the CTL models.

We found that only four habitable planets have $t_{\rm lock}$ between 0.1 Gyr and 1 Gyr, namely LP 834–042 d (Astudillo-Defru et al. 2017b), PM J11293-0127 d (Almenara et al. 2015; Sinukoff et al. 2016), HD 156384 C e (Anglada-Escudé et al. 2013), and CD–44 11909 c (Tuomi et al. 2014), and 9 greater than 1 Gyr, GJ 96 b (Hobson et al. 2018), CD–23 1056 b (Forveille et al. 2011), BD–06 1339 c (Lo Curto et al. 2013), Ross 1003 b (Trifonov et al. 2018), HD 147379 b (Reiners et al. 2018), V1428 Aql b (Kaminski et al. 2018), Kepler-186 f (Torres et al. 2015), and IL Aqr b and c (Trifonov et al. 2018). In this situation, all of them could host exomoons beyond the Roche limit after all the material in the protoplanetary disk is dissipated (10–30 Myr, Bertout 1989; Hartmann et al. 1998; Calvet et al. 2002). All other habitable planets get tidally locked in less than 90 Myr.

However, the moon migration timescales are too low. In this scenario, only for six habitable exoplanets the condition $a_m > a_{\rm Roche}$ holds. The migration timescales are greater than $t_{\rm H}$, being $t_{\rm H} = 14.4$ Gyr the Hubble time (which is slightly longer than the universe age at 13.8 Gyr), for four exoplanets (CD–23 1056 b, Forveille et al. 2011; Ross 1003 b, Haghighipour et al. 2010; Trifonov et al. 2018; IL Aqr b and c, Trifonov et al. 2018), whose properties are shown in the top part of Table 4 and discussed in Section 3.3. The four of them have $a_m > a_{{\rm crit},m} > a_{\rm Roche}$, the largest planetary radii in the HZ ($R_p = 12$–$14\,R_\oplus$), and $\tau_{\rm mig} \gg 0.8$ Gyr, which was the Earth's Late Heavy Bombardment duration (Fassett & Minton 2013; Norman & Nemchin 2014). In this $P_{0,1} = P_{\rm orb}$ scenario, the hypothetical moons around the other 29 planets would fall onto them on timescales much shorter than protoplanetary disk

[11] $a_{\rm Moon} = 3.84399 \times 10^8$ m, $M_{\rm Moon} = 7.346 \times 10^{22}$ kg, and $R_\oplus = 6.3781366 \times 10^6$ m.

[12] https://github.com/RoryBarnes/EqTide

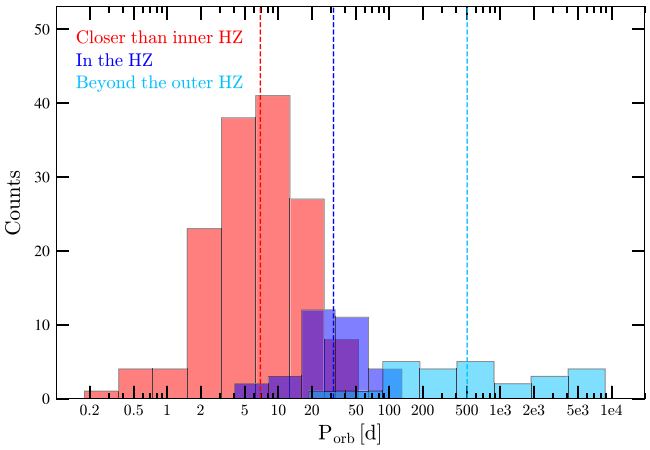

Figure 3. Orbital periods for the exoplanets in our sample. The colors are the same as those in Figure 2. The dashed, vertical lines show the median period for each subgroup.

Table 2
Love Number, Tidal Quality Factor, and Radius of Gyration for Different Planetary Types

Planet Type	k_2	Q	λ
Dry telluric	0.5	100	0.370
Terran	0.3	12	0.330
Icy Neptunian	1.5	10^4	0.230
Gaseous Jovian	1.5	10^6	0.254

Table 3
Parameters for Deriving k_2 (Equation (8)), Q (Equation (9)), and λ (Equation (10))

R_p	$k_{2,0}$	γ $(R_\oplus^{-1})$	Q_0 $(R_\oplus^{-\delta})$	δ	λ_0	ϵ $(R_\oplus^{-1})$
$\leqslant$1.50	0.3	0	10^2	0	0.37	0
1.50–3.88	−0.456	0.504	14.019	4.846	0.458	−0.059
3.88–10.97	1.5	0	24.600	4.431	0.217	0.003
10.97–26	1.5	0	10^6	0	0.254	0

dissipation times under the EqTide layout, not counting potential viscosity in the protomoon disk (Lin & Papaloizou 1986; Pollack et al. 1996; Montmerle et al. 2006; Sasaki et al. 2010). The fifth and sixth habitable exoplanets for which $a_m > a_{\rm Roche}$, LP 834–042 b and BD–06 1339 c, have short $\tau_{\rm mig}$ of about 50 and 18 Myr, respectively, which are comparable to the typical protoplanetary disk dissipation time (Ida & Lin 2004; Hernández et al. 2007; Lambrechts & Johansen 2012).

On the other hand, $P_{0,2} = 3.0$ hr ($\tau_{{\rm mig},m} \propto Q\ R_{\rm p}^{27} M_{\rm p}^{8}$) is the smallest value used by Piro (2018), similar to the shortest $P_{\rm orb}$ in our sample ($P_{0,2} \approx 4.13$ hr, K2-137 b), which is close to its star and far from the HZ boundary, and probably near the shortest allowed value of P_0 (see below). The value of 3.0 hr is also lower than the sidereal rotation periods of Jupiter and Saturn (9.925 and 10.55 hr, respectively), and might be unrealistic in the context of this work. Contrary to the $P_{0,1} = P_{\rm orb}$ scenario, all moons are stripped away (which means that $\tau_{{\rm mig},m} \propto Q\ R_{\rm p}^{-5} M_{\rm p}^{8/3} M_*^{-8/3}$), but with migration

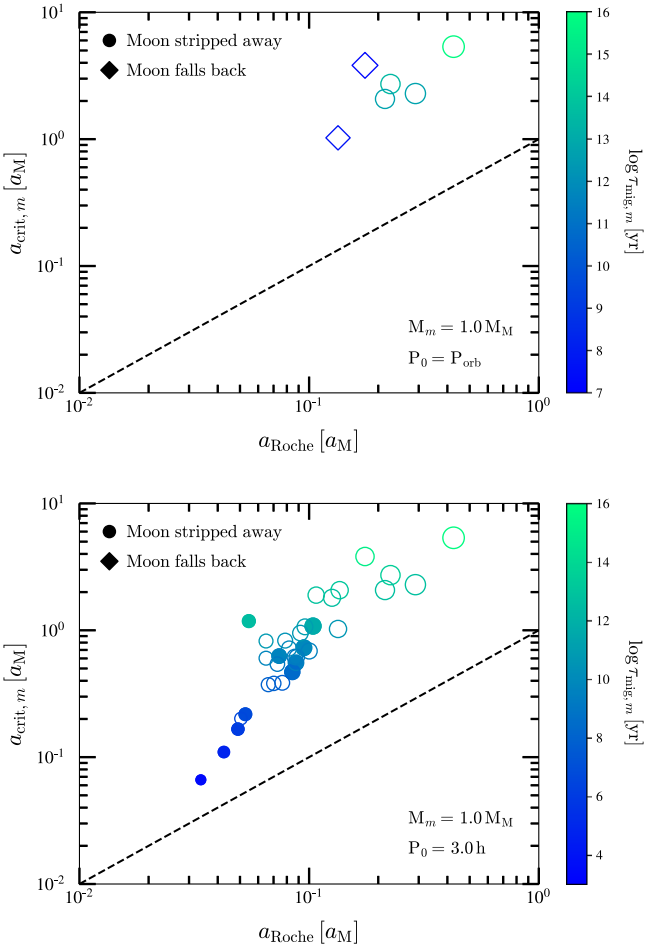

Figure 4. $a_{{\rm crit},m}$ vs. $a_{\rm Roche}$ for the modeled exomoons around all the potentially habitable exoplanets in our sample. The circles and the squares (filled for primary transit exoplanet detection, empty for RV exoplanet detection) represent an exomoon being stripped away by the host star or falling back into the exoplanet, respectively. They are depicted with sizes proportional to their exoplanet hosts' masses in logarithmic scale. The black, dashed line corresponds to the exomoon tidal disruption limit, so no exomoon can exist below it. Top: $P_0 = P_{\rm orb}$ for each planet. Bottom: $P_0 = 3.0$ hr.

timescales greater than 0.8 Gyr for 26 planet–moon systems, including the four systems in Table 4. Of them, 15 planet–moon systems have $\tau_{\rm mig} > t_{\rm H}$. They are GJ 96 b (Hobson et al. 2018), CD–23 1056 b (Stassun et al. 2017), LP 834–042 b (Astudillo-Defru et al. 2017b), LP 834–042 d (Astudillo-Defru et al. 2017b), Kapteyn's star b (Anglada-Escudé et al. 2014), BD–06 1339 c (Lo Curto et al. 2013), PM J11293–0127 d (Almenara et al. 2015; Sinukoff et al. 2016), Ross 1003 b (Trifonov et al. 2018), HD 147379 b (Reiners et al. 2018), HD 156384 C e (Anglada-Escudé et al. 2013), CD–44 11909 c (Tuomi et al. 2014), V1428 Aql b (Kaminski et al. 2018), Kepler-186 f (Torres et al. 2015), and IL Aqr b and c (Trifonov et al. 2018). However, except for nine cases, GJ 96 b, CD–23 1056 b, BD–06 1339 c, Ross 1003 b, HD 147379 b, V1428 Aql b, Kepler-186 f, and IL Aqr b and c, all tidal locking times are shorter than 0.8 Gyr ($t_{\rm lock} \ll \tau_{{\rm mig},m}$), which actually transforms this scenario into the previous one, $P_{0,1} = P_{\rm orb}$. For the four planets listed in Table 4, the migration timescales remain unscathed, as $a_m > a_{{\rm crit},m}$.

To better understand the values of the exomoon migration timescales, we calculated the maximum and minimum allowed $\tau_{{\rm mig},m}$, i.e., we substituted $a_m = a_{{\rm crit},m}$ and $a_m = a_{\rm Roche}$ in

Table 4
Potentially Habitable Exoplanets That Can Host Exomoons

Planet	GJ	a (au)	$P_{\rm orb}$ (days)	M_* ($M_\odot$)	$M_{\rm p}$ ($M_\oplus$)	$R_{\rm p}$ ($R_\oplus$)	a_m ($a_{\rm M}$)	$a_{\rm Roche}$ ($a_{\rm M}$)	$a_{{\rm crit},m}$ ($a_{\rm M}$)	$\tau_{{\rm mig},m}$ (Gyr)	$P_{{\rm orb},m}$ (days)	$Q_{\rm tidal}$ (TW)
CD-23 1056 b	…	0.25	53.435	0.62	>114.0	(>13.2)	2.72	0.23	2.72	$>t_{\rm H}$	⩽11.0	$\lesssim$7
Ross 1003 b	1148	0.17	41.38	0.35	>96.7	(>12.0)	2.08	0.21	2.08	$>t_{\rm H}$	⩽8.0	$\lesssim$32
IL Aqr b	876	0.21	61.082	0.34	>760.9	(>13.3)	5.36	0.43	5.36	$>t_{\rm H}$	⩽11.8	$\lesssim$5
IL Aqr c	876	0.13	30.126	0.34	>241.5	(>14.0)	2.29	0.29	2.29	$>t_{\rm H}$	⩽5.9	$\lesssim$126

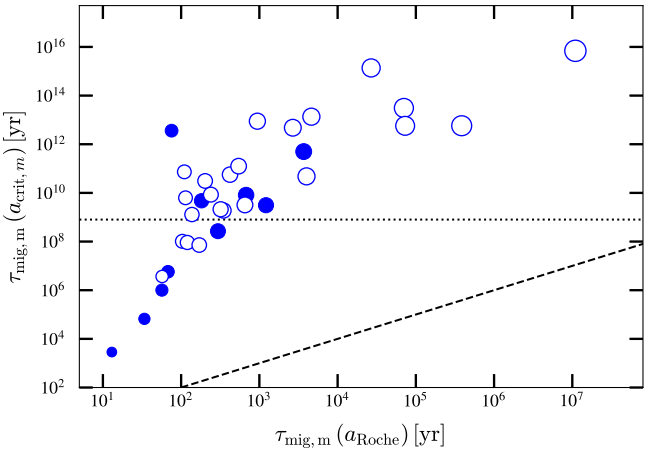

Figure 5. Maximum vs. minimum allowed values of exomoon migration timescales for the potentially habitable exoplanets in our sample. The points are depicted with sizes proportional to the exoplanets' masses in logarithmic scale. The black, dashed line corresponds to the most extreme case, $a_{{\rm crit},m} = a_{\rm Roche}$. The black, dotted, horizontal line shows the 0.8 Gyr boundary mentioned in the text (the Earth's Late Heavy Bombardment).

Equation (4), respectively. Figure 5 shows the range of $\tau_{{\rm mig},m}$ for the potentially habitable exoplanets in our sample. In principle, all the 24 exoplanets above the Earth's Late Heavy Bombardment line might host exomoons. However, the parameter space is only broad enough for the five exoplanets on the upper right side of Figure 5, which are the four planets listed in Table 4 and BD–06 1339 c. We compared our migration timescales for these five most extreme cases with the values resulting from applying the numerical technique of Piro (2018) by varying the planet–moon separation over an allowable range and the spin of the planet, and found that our values are slightly longer than, but comparable to, these. We kept our values for consistency.

3.3. Potentially Habitable Exomoons

As presented in Section 3.2, only four potentially habitable exoplanets might be able to host exomoons for timescales above 0.8 Gyr under the $P_0 = P_{\rm orb}$ scenario: CD–23 1056b (a giant exoplanet around an active, metal-rich, M0.0 V star in Eridanus–Forveille et al. 2011), IL Aqr b,c (two giant exoplanets around a nearby M4.0 V star with a four-planet system—Delfosse et al. 1998; Marcy et al. 1998, 2001; Trifonov et al. 2018), and Ross 1003b (an eccentric, Saturn-mass planet around a nearby M4.0 V star with a multiplanetary system[13]—Haghighipour et al. 2010; Trifonov et al. 2018). The four planets are relatively large and have minimum masses between 0.30 and 2.39 $M_{\rm Jup}$ (i.e., between 97 and 761 $M_\oplus$).

We analyzed the effects of tidal heating $Q_{\rm tidal}$ (e.g., Barnes et al. 2008; Jackson et al. 2008a, 2008b, 2008c) on the four exomoons to assess if their mantles would melt, which, for a rocky body, occurs if $Q_{\rm tidal} \gtrsim 100$ TW (Moore et al. 2007; Lainey et al. 2009; Veeder et al. 2012; Driscoll & Barnes 2015). Barnes & Heller (2013) defined four categories of Earth-mass exoplanets in the HZ depending on the tidal heating that they experience: "Earth twins" ($Q_{\rm tidal} < 20$ TW), "Tidal Earths" (20 TW $< Q_{\rm tidal} <$ 1020 TW), "Super-Ios" (1020 TW $< Q_{\rm tidal} <$ 134000 TW), and "Tidal Venuses" ($Q_{\rm tidal} >$ 134000 TW). We estimated $Q_{\rm tidal}$ for each exoplanet–exomoon system by means of the publicly available `VPLanet`[14] code (Barnes et al. 2016, 2018, 2019), modifying the example `IoHeat`. So far, we had assumed zero eccentricity and obliquity, as in Piro (2018), in which case tidal heating can only come from rotation, assuming that it is not synchronous. Hence, we relaxed this condition and set a small value for the eccentricity $e = 0.01$. We also assumed that the exomoon is tidally locked to the exoplanet. As $Q_{\rm tidal}$ is directly proportional to the moon's size, we took a Ganymede-like exomoon to estimate an upper limit for the tidal heating (Ganymede is the biggest solar system moon).[15] We set the exomoon's semimajor axis a_m to the mean distance between the Roche limit and the Hill radius from Table 4. We let each system evolve for $t = 10^4$ years and found that only a potential exomoon around IL Aqr c might reach the mantle melting threshold. We report the upper limit for $Q_{\rm tidal}$ in Table 4.

Some of these moons might be detected with current and near-future technology. The detectability of moons by the transit method (or, more likely, photocentric transit timing variation) has been extensively and intensively discussed in the literature (Sartoretti & Schneider 1999; Barnes & O'Brien 2002; Szabó et al. 2006; Pont et al. 2007; Kipping 2009; Kipping et al. 2014; Hippke & Angerhausen 2015; Simon et al. 2015; Perryman 2018). The ESA space mission (*CHEOPS*; Fortier et al. 2014) might discover moons with the transit method around the brightest M dwarfs, while, if the moons were massive and dense enough, ESPRESSO at the Very Large Telescope (Pepe et al. 2010) could also detect the modification of the amplitude and signature of the Rossiter–McLaughlin effect as in Zhuang et al. (2012). Unfortunately, none of the four planets in the stars' HZ with long moon migration times transits. If the NASA space mission *TESS*, currently in operation (Ricker et al. 2014), discovered additional M-dwarf planets in this class, but transiting, they should be a high priority target for ESPRESSO or any other ultra-stable spectrograph with cm s^{-1} accuracy at a large telescope.

Regarding the potential habitability of these Moon-mass exomoons, they may not retain an atmosphere at 300 K due to

[13] In the last stages of revision of this paper, we became aware of an independent study of the exomoon hypothesis around Ross 1003, by T. Trifonov et al. (2019, in preparation).

[14] https://github.com/VirtualPlanetaryLaboratory/vplanet

[15] $M_{\rm Gan} = 1.48 \times 10^{23}$ kg; $R_{\rm Gan} = 2.6341 \times 10^6$ m.

their low gravities. As Titan is less than twice as massive ($1.83\,M_{\rm M}$), increasing the exomoon mass to Titan's would not significantly affect our results; the condition $a_m > a_{{\rm crit},m}$ for the four systems in Table 4 would still be met. The minimum mass to hold onto an atmosphere in the HZ of a star is not known, but is probably close to Mars' ($8.71\,M_{\rm M}$, Pollack et al. 1987; Selsis et al. 2007). If we increased the masses of our putative exomoons to Mars' mass, then, for the four systems in Table 4, $\tau_{{\rm mig},m}$ would be of the order of 5 million years for CD-23 1056b and Ross 1003b, and would lie above the Hubble time for IL Aqr b anc c. These four systems would remain near the upper right corner of Figure 5, indicating that their $\tau_{{\rm mig},m}$ values are sufficiently long to still permit a long lifetime.

4. Conclusions

First of all, we compiled orbital, astrometric, photometric, and basic astrophysical parameters of a comprehensive list of 205 exoplanets around 109 M dwarfs discovered with the radial velocity or transit methods. We calculated the most probable masses and radii of 192 planets using the models of Chen & Kipping (2017), and assumed literature values for the other 13 planets with both radial velocity and transit measurements. For all 109 host stars, we derived luminosities, effective temperatures, and masses from public photometric catalogs, BT-Settl CIFIST models of the Lyon group, the Virtual Observatory Spectral energy distribution Analyzer, a near-infrared absolute magnitude-mass relation, and, except for only two cases, *Gaia* parallaxes.

With the available data, for every star we outlined the inner and outer HZ boundaries from a one-dimensional climate model. There are 33 known planets that orbit within the HZ limits of M dwarfs. Despite being tidally locked to their (active) host stars in most cases, it may still be possible for these planets to retain the conditions for habitability. In this scenario, even if most of the planets in the HZ might not host liquid water, because they are icy Neptunians, some of their hypothetical exomoons could instead.

For each of the 33 planets, we modeled noneccentric, nonobliquous moons, and computed moon migration timescales for two different scenarios: strip-away from the planet, and fall back onto the planet. We also considered two extreme cases for the initial planetary spin: a maximum value corresponding to the orbital period (i.e., the planet is tidally locked), and a minimum value of 3 hr. In the $P_0 = P_{\rm orb}$ scenario, all hypothetical moons fall back onto their planets after short timescales, except for four planets whose migration timescales are longer than the Hubble time (Ross 1003b, IL Aqr b and c, and CD–23 1056b). Only for these cases a hypothetical moon could be stable for timescales longer than protoplanetary disk dissipation times. We also explored the effects of tidal heating in the exomoons, in particular, if their mantles would partially melt, similar to Io in the solar system. All our code is publicly available in a GitHub repository[16] and archived in Zenodo (doi.10.5281/zenodo.3533659).

Our planet compilation dates back to 2019 March 19. As a future work, a new M-dwarf exoplanet list should be updated with recent discoveries, such as Teegarden's b and c (Zechmeister et al. 2019) and, especially, the transiting warm Earth-mass planet GJ 357 b (Luque et al. 2019). Besides, the stellar mass determination could be improved with the new luminosity–radius–mass relation of Schweitzer et al. (2019) or, more interestingly, for studying the long-term stability of hypothetical moons, direct *N*-body analyses could be carried out.

H.M.-R. acknowledges support from a PITT PACC, a Zaccheus Daniel and a Kenneth P. Dietrich School of Arts & Sciences Predoctoral Fellowship from the Department of Physics and Astronomy at the University of Pittsburgh. J.A.C. and C.C. acknowledge financial support from the Agencia Estatal de Investigación of the Ministerio de Ciencia, Innovación y Universidades and the European FEDER/ERF funds through projects AYA2016-79425-C3-2-P, BES-2017-080769, and MDM-2017-0737. R.B. was supported by the NASA Virtual Planetary Laboratory Team through grant No. 80NSSC18K0829. This work also benefited from participation in the NASA Nexus for Exoplanet Systems Science research coordination network. This research has made use of NASA's Astrophysics Data System Bibliographic Services, the VizieR catalog access tool, VOSA, which is developed under the Spanish Virtual Observatory project supported from the Spanish MINECO through grant AYA2017-84089, and the NASA Exoplanet Archive, which is operated by the California Institute of Technology, under contract with the National Aeronautics and Space Administration under the Exoplanet Exploration Program.

Software: `SciPy` (Virtanen et al. 2019), `Matplotlib` (Hunter 2007), `IPython` (Pérez & Granger 2007), `Numpy` (Van Der Walt et al. 2011), `Astropy` (Astropy Collaboration et al. 2013; Price-Whelan et al. 2018), `EqTide` (Barnes et al. 2016; Barnes 2017), `VPLanet` (Barnes et al. 2016, 2018, 2019).

Appendix
Long Tables

Table 5 reproduces the basic properties of planet-host M dwarfs. Table 6 reproduces the basic properties of M-dwarf hosted exoplanets.

[16] https://github.com/hector-mr/Exomoons_HZ_Mdwarfs/

Table 5
Basic Properties of Planet-host M Dwarfs

Name	Alternative Names	α[a]	δ[a]	d[b] (pc)	Sp. Type	$T_{\rm eff}$[c] (K)	L[c] ($10^{-4}\,L_{\odot}$)	M_{*}[d] ($M_{\odot}$)
GX And	GJ 15A	00:18:27.04	+44:01:29.0	3.563 ± 0.001	M1.0 V	3600	253.6 ± 4.0	0.40
K2-149	EPIC 220522664	00:39:17.22	+07:16:37.2	124.1 ± 0.5	M1 V	3700	677 ± 17	0.59
CD-44 170	GJ 27.1	00:39:59.52	−44:15:15.0	23.62 ± 0.03	M0.5 V	3700	459.7 ± 8.7	0.52
LHS 1140	GJ 3053	00:44:59.67	−15:16:26.8	14.99 ± 0.02	M4.5 V	3100	44.25 ± 0.55	0.18
2MASS J01021226-6145216	HATS-71	01:02:12.45	−61:45:22.1	140.79 ± 0.86	M3.0 V	3300	251.9 ± 5.5	0.45
BD+61 195	GJ 49	01:02:40.50	+62:20:43.6	9.856 ± 0.003	M1.5 V	3600	452.4 ± 9.5	0.54
YZ Cet	GJ 54.1	01:12:31.94	−16:59:46.5	3.712 ± 0.001	M4.5 V	3100	22.00 ± 0.35	0.14
K2-150	EPIC 220598331	01:13:22.65	+08:59:14.8	102.8 ± 0.8	M2.5 V	3400	224.3 ± 5.5	0.41
K2-151	EPIC 220621087	01:17:13.15	+09:30:04.6	69.6 ± 0.2	M1.5 V	3700	326.2 ± 4.6	0.46
BD-17 400	GJ 3138	02:09:11.46	−16:20:21.3	28.49 ± 0.03	M0 V	3900	835 ± 13	0.61
GJ 96	G 173-53	02:22:14.98	+47:52:48.8	11.936 ± 0.009	M0 V	3900	638.6 ± 9.4	0.58
CD-23 1056	LTT 1349	02:46:43.22	−23:05:09.6	23.39 ± 0.02	M0 V	4000	908 ± 13	0.62
LP 413-32 B	K2-288 B	03:41:46.63	+18:16:06.6	65.72 ± 0.87	M3.0 V	3200	364 ± 18	0.50
BD-21 784	GJ 160.2	04:06:34.90	−20:51:23.3	25.88 ± 0.04	K7 V	4300	1372 ± 22	0.65
LPM 178	GJ 163	04:09:17.48	−53:22:16.2	15.135 ± 0.007	M3.5 V	3400	217.0 ± 3.7	0.41
Melotte 25 VA 50	K2-25	04:13:05.74	+15:14:51.7	45.0 ± 0.2	M4.5 V	3200	77.6 ± 1.3	0.27
HG 8-15	K2-155	04:21:52.48	+21:21:12.9	73.0 ± 0.3	M0.0 V	3500	998 ± 15	0.66
LP 834-042	GJ 3293	04:28:35.63	−25:10:16.8	20.20 ± 0.02	M2.5 V	3500	275.8 ± 3.9	0.45
LEHPM 3808	TOI-270	04:33:39.86	−51:57:26.6	22.49 ± 0.01	M3.0 V	3500	167.6 ± 2.8	0.36
LP 358-499	K2-133	04:40:35.85	+25:00:35.3	75.3 ± 0.2	M1 V	3800	351.3 ± 4.2	0.46
HD 285968	GJ 176	04:42:56.49	+18:57:12.1	9.473 ± 0.006	M2.0 V	3500	364.8 ± 7.3	0.49
Wolf 1539	GJ 179	04:52:05.89	+06:28:30.8	12.360 ± 0.009	M3.5 V	3300	157.6 ± 3.0	0.37
LPM 198	GJ 180	04:53:50.42	−17:46:34.3	11.945 ± 0.004	M2.0 V	3500	242.7 ± 3.6	0.41
LP 656-38	GJ 3323	05:01:56.85	−06:56:54.6	5.376 ± 0.002	M4 V	3100	36.54 ± 0.53	0.17
Kapteyn's	GJ 191	05:11:50.08	−45:02:34.9	3.9335 ± 0.0004	M0 V	3700	128.1 ± 3.5	0.38
LP 892-26	GJ 3341	05:15:47.31	−31:17:41.4	23.64 ± 0.03	M2.5 V	3500	321.5 ± 5.1	0.47
NGTS-1	…	05:30:51.41	−36:37:51.5	219.5 ± 1.0	M0.5 V	3900	679 ± 14	0.57
HATS-6	…	05:52:35.23	−19:01:53.9	170.1 ± 1.1	M1 V	3800	702 ± 15	0.59
BD-06 1339	GJ 221	05:52:59.70	−05:59:49.0	20.28 ± 0.02	K7 V	4100	1039 ± 24	0.63
HD 42581	GJ 229A	06:10:34.46	−21:52:03.8	5.757 ± 0.002	M0.5 V	3700	542 ± 28	0.55
PM J06168+2435	K2-26	06:16:49.54	+24:35:45.0	99.3 ± 0.5	M1 V	3700	443.5 ± 9.0	0.52
Luyten's star	GJ 273	07:27:25.09	+05:12:35.6	3.80 ± 0.02	M3.5 V	3200	99.0 ± 3.5	0.29
LP 424-4	GJ 3470	07:59:05.64	+15:23:28.4	29.45 ± 0.05	M1.5 V	3500	400.5 ± 4.9	0.50
NGC 2632 JS 183	K2-95	08:37:27.02	+18:58:35.8	180.7 ± 4.0	M3 V	3400	219 ± 11	0.41
K2-146	EPIC 211924657	08:40:06.41	+19:05:32.4	79.5 ± 0.5	M3 V	3300	123.6 ± 2.7	0.31
LP 844-8	GJ 317	08:40:58.69	−23:27:10.1	15.203 ± 0.013	M3.5	3300	224.1 ± 3.8	0.42
NGC 2632 JS 597	EPIC 211964830	08:45:26.00	+19:41:54.2	186.6 ± 2.1	M2 V	3500	317.1 ± 9.5	0.47
BD+02 2098	GJ 328	08:55:07.67	+01:32:31.2	20.54 ± 0.02	M0.0 V	3900	995 ± 12	0.63
K2-117	EPIC 211331236	08:55:25.38	+10:28:09.2	101.9 ± 0.4	M1.0 V	3700	444.4 ± 9.4	0.52
BD+48 1829	GJ 378	10:02:20.77	+48:04:56.8	14.96 ± 0.01	M1.0 V	3700	577 ± 10	0.56
LTT 3758	GJ 1132	10:14:50.18	−47:09:17.8	12.618 ± 0.007	M4.5 V	3200	46.53 ± 0.58	0.19
K2-239	EPIC 248545986	10:42:22.59	+04:26:28.9	31.11 ± 0.08	M3.0 V	3400	71.90 ± 0.94	0.23
LP 905-36	GJ 3634	10:58:34.40	−31:08:39.6	20.39 ± 0.03	M2.5 V	3500	288.4 ± 4.5	0.46
Lalande 21185	GJ 411	11:03:20.19	+35:58:11.6	2.547 ± 0.004	M1.5 V	3400	185 ± 13	0.41
Innes' star	GJ 422	11:15:55.45	−57:32:33.2	12.668 ± 0.007	M3.5 V	3400	179.0 ± 2.5	0.36
K2-22	EPIC 201637175	11:17:55.85	+02:37:08.5	245.5 ± 2.8	M0 V	3900	810 ± 30	0.61
PM J11293-0127	K2-3	11:29:20.49	−01:27:18.5	44.1 ± 0.1	M0 V	3900	603 ± 12	0.55
PM J11302+0735	K2-18	11:30:14.43	+07:35:16.2	38.07 ± 0.08	M2.5 V	3500	264.0 ± 4.2	0.44
CD-31 9113	GJ 433	11:35:26.86	−32:32:37.1	9.067 ± 0.004	M1.5 V	3600	339.5 ± 5.2	0.47
Ross 1003	GJ 1148	11:41:43.83	+42:45:05.7	11.018 ± 0.006	M4 V	3200	149.9 ± 1.7	0.35
Ross 905	GJ 436	11:42:12.13	+26:42:11.0	9.756 ± 0.009	M2.5 V	3300	238.9 ± 3.5	0.42
LP 613-39	K2-9	11:45:03.29	+00:00:19.5	83.2 ± 0.4	M2.5 V	3500	121.7 ± 2.0	0.30
FI Vir	GJ 447	11:47:45.02	+00:47:57.4	3.375 ± 0.001	M4 V	3100	38.27 ± 0.56	0.18
K2-152	EPIC 201128338	12:06:31.78	−05:49:38.8	108.8 ± 0.4	M0 V	3900	886 ± 16	0.61
K2-153	EPIC 201598502	12:15:14.13	+02:01:15.2	143.7 ± 0.9	M3.0 V	3800	535 ± 12	0.54
K2-137	EPIC 228813918	12:27:28.90	−06:11:42.8	99.2 ± 0.6	M3 V	3500	283.0 ± 6.1	0.46
K2-154	EPIC 228934525	12:36:00.36	−02:40:10.6	129.8 ± 0.4	M0 V	3900	983 ± 16	0.63
Ross 1020	GJ 3779	13:22:56.05	+24:27:50.2	13.749 ± 0.012	M4.0 V	3300	82.2 ± 1.0	0.25
HD 122303	GJ 536	14:01:02.33	−02:39:08.2	10.412 ± 0.009	M1 V	3700	433.5 ± 7.2	0.51
Proxima Centauri	GJ 551	14:29:34.43	−62:40:34.3	1.3012 ± 0.0003	M5.5 V	2800	15.37 ± 0.39	0.12
K2-240	EPIC 249801827	15:11:23.85	−17:52:31.6	73.1 ± 0.5	M0.5 V	3800	628 ± 15	0.57
HO Lib	GJ 581	15:19:25.55	−07:43:21.7	6.299 ± 0.002	M3 V	3400	120.0 ± 1.7	0.31
K2-286	EPIC 249889081	15:33:28.76	−16:46:25.4	76.32 ± 0.23	M0 V	4000	904 ± 12	0.62

Table 5
(Continued)

Name	Alternative Names	α[a]	δ[a]	d[b] (pc)	Sp. Type	$T_{\rm eff}$[c] (K)	L[c] ($10^{-4}\,L_{\odot}$)	M_{*}[d] ($M_{\odot}$)
MCC 759	GJ 3942	16:09:03.49	+52:56:38.9	16.937 ± 0.006	M0 V	3800	646.2 ± 7.3	0.57
USco J161014.7-191909	K2-33	16:10:14.73	−19:19:09.8	139.8 ± 1.5	M3 V	3100	1019 ± 32	0.70
LP 804-27	HIP 79431	16:12:41.82	−18:52:35.1	14.54 ± 0.03	M3 V	3400	301.8 ± 5.9	0.48
HD 147379	GJ 617A	16:16:41.42	+67:14:21.1	10.768 ± 0.004	M0.0 V	3900	978 ± 23	0.63
MCC 767	GJ 625	16:25:25.39	+54:18:12.1	6.474 ± 0.001	M2.0 V	3500	148.1 ± 2.1	0.32
V2306 Oph	GJ 628	16:30:17.96	−12:40:03.7	4.306 ± 0.001	M3.5 V	3300	108.2 ± 1.6	0.30
BD+25 3173	GJ 649	16:58:08.72	+25:44:31.1	10.383 ± 0.003	M1.5 V	3700	434.4 ± 4.6	0.52
LHS 3275	GJ 1214	17:15:19.54	+04:57:38.4	14.65 ± 0.04	M4.5 V	3000	38.85 ± 0.50	0.18
BD+11 3149	GJ 3998	17:16:00.49	+11:03:22.2	18.16 ± 0.02	M1.0 V	3700	467 ± 12	0.52
HD 156384 C	GJ 667C	17:19:00.25	−34:59:52.0	7.245 ± 0.005	M1.5 V	3500	149.5 ± 2.3	0.33
CD-46 11540	GJ 674	17:28:40.81	−46:53:56.3	4.550 ± 0.001	M2.5 V	3400	167.4 ± 3.0	0.35
CD-51 10924	GJ 676A	17:30:10.77	−51:38:16.0	16.035 ± 0.010	M0 V	3900	900 ± 16	0.63
BD+68 946	GJ 687	17:36:25.00	+68:20:01.2	4.550 ± 0.001	M3.0 V	3400	221.1 ± 4.9	0.40
CD-44 11909	GJ 682	17:37:02.65	−44:19:23.7	5.007 ± 0.002	M3.5 V	3200	81.18 ± 0.77	0.27
BD+18 3421	GJ 686	17:37:54.36	+18:35:45.4	8.159 ± 0.002	M1.5 V	3700	277 ± 18	0.44
Barnard's star	V2500 Oph	17:57:48.49	+04:41:40.5	1.827 ± 0.001	M3.5 V	3200	35.58 ± 0.72	0.16
Kepler-83	KOI-898	18:48:55.80	+43:39:56.0	405.0 ± 5.2	M0 V	4100	919 ± 30	0.61
Kepler-446	KOI-2842	18:49:00.03	+44:55:15.6	96.6 ± 0.5	M4 V	3400	49.74 ± 0.98	0.19
Kepler-303	KOI-1515	18:52:32.51	+43:39:24.1	211.0 ± 0.9	M0 V	4100	876 ± 18	0.61
Kepler-617	KOI-596	18:54:57.77	+47:30:58.1	174.2 ± 1.0	M1 V	3700	512.3 ± 9.2	0.55
Kepler-236	KOI-817	18:55:27.94	+39:53:53.5	291.2 ± 2.3	M1 V	3900	755 ± 18	0.60
Kepler-235	KOI-812	19:04:18.98	+39:16:41.7	433.2 ± 6.7	M0 V	4100	880 ± 34	0.61
Kepler-52	KOI-775	19:06:57.12	+49:58:32.7	324.5 ± 2.4	M0 V	4200	1053 ± 25	0.63
Kepler-155	KOI-438	19:13:58.99	+51:04:54.9	296.0 ± 2.3	K7 V	4400	1726 ± 58	0.68
V1428 Aql	GJ 752A	19:16:54.66	+05:09:47.4	5.912 ± 0.002	M2.5 V	3500	325.8 ± 4.0	0.47
Kepler-138	KOI-314	19:21:31.54	+43:17:35.0	67.0 ± 0.1	M1 V	3900	575.7 ± 7.5	0.54
LSPM J1928+4437	Kepler-42	19:28:52.70	+44:37:02.5	40.11 ± 0.06	M4 V	3400	29.01 ± 0.36	0.14
Kepler-49	KOI-248	19:29:10.68	+40:35:30.5	314.0 ± 2.5	M1 V	4000	946 ± 23	0.62
LSPM J1930+4149	Kepler-1649	19:30:00.71	+41:49:48.0	92.4 ± 0.5	M4: V	3300	52.4 ± 1.0	0.20
Kepler-45	KOI-254	19:31:29.50	+41:03:51.0	386.0 ± 6.5	M1 V	3800	807 ± 34	0.61
Kepler-231	KOI-784	19:35:53.61	+50:31:54.7	319.5 ± 3.3	M1 V	4100	818 ± 26	0.59
Kepler-54	KOI-886	19:39:05.74	+43:03:22.3	273.8 ± 2.9	M1 V	3800	480 ± 14	0.53
Kepler-252	KOI-912	19:42:19.04	+44:32:45.3	383.6 ± 3.5	M0 V	4300	1421 ± 42	0.67
Kepler-32	KOI-952	19:51:22.15	+46:34:27.7	326.9 ± 3.4	M1 V	3900	650 ± 19	0.57
Kepler-125	KOI-251	19:53:01.95	+47:36:18.0	184.3 ± 1.0	M1 V	3800	558.7 ± 9.6	0.55
Kepler-186	KOI-571	19:54:36.66	+43:57:18.0	178.5 ± 0.8	M1 V	3900	571 ± 14	0.55
Kepler-445	KOI-2704	19:54:56.72	+46:29:56.8	127.7 ± 1.0	M4 V	3200	77.6 ± 2.1	0.28
Kepler-267	KOI-1078	19:59:19.34	+47:09:27.3	267.0 ± 2.5	M1 V	3900	584 ± 16	0.55
HD 204961	GJ 832	21:33:33.90	−49:00:45.1	4.965 ± 0.001	M1.5 V	3600	292 ± 11	0.44
BD-05 5715	GJ 849	22:09:41.52	−04:38:27.0	8.803 ± 0.004	M3.5 V	3400	282.5 ± 4.2	0.47
LP 819-052	GJ 1265	22:13:43.79	−17:41:13.4	10.255 ± 0.007	M4.5 V	3100	36.35 ± 0.46	0.17
LP 700-6	K2-28	22:22:29.60	−07:57:22.9	63.1 ± 0.3	M4 V	3200	116.8 ± 2.3	0.33
K2-21	EPIC 206011691	22:41:12.91	−14:29:21.6	83.8 ± 0.3	M0 V	4100	978 ± 14	0.63
LHS 3844[e]	LEHPM 5027	22:41:59.09	−69:10:19.6	14.891 ± 0.011	m4:	3000	27.10 ± 0.29	0.16
IL Aqr	GJ 876	22:53:17.75	−14:15:59.7	4.676 ± 0.002	M4.0 V	3200	129.3 ± 3.0	0.34
2MUCD 12171	TRAPPIST-1	23:06:30.33	−05:02:36.5	12.43 ± 0.02	M8.0 V	2500	5.38 ± 0.06	0.09

Notes.
[a] All equatorial coordinates are given in the epoch of *Gaia* DR2 (J2015.5) (Gaia Collaboration et al. 2016), except for Luyten's star and Lalande 21185, with equatorial coordinates given in the epoch of 2MASS (J2000) (Skrutskie et al. 2006).
[b] All distances calculated using parallaxes from *Gaia* DR2 (Gaia Collaboration et al. 2016, 2018), except for Luyten's star and Lalande 21185, calculated using parallaxes from *Hipparcos* (van Leeuwen 2007).
[c] L and $T_{\rm eff}$ computed with VOSA (Bayo et al. 2008) from our compiled photometry. The uncertainties in the effective temperatures are $\delta T_{\rm eff} = 50$ K in all cases.
[d] Stellar masses calculated from K_s apparent magnitudes, tabulated distances, and the relations of Mann et al. (2019), as in Schweitzer et al. (2019).
[e] Spectral type of LHS 3844 estimated from its photometric data.

(This table is available in machine-readable form.)

Table 6
Basic Properties of M-dwarf Hosted Exoplanets

Name	Planet	a (au)	P_{orb} (days)	M_p[a] ($M_\oplus$)	R_p[a] ($R_\oplus$)	References[b]	S_{eff} ($S_\odot$)	$T_{eq,p}$ (K)	Potentially HZ
GX And	b	$0.072^{+0.003}_{-0.004}$	$11.4407^{+0.0017}_{-0.0016}$	$>3.03^{+0.46}_{-0.44}$	(>1.53)	Pin18	4.89 ± 0.10	413.9 ± 8.7	⋯
K2-149	b	$0.083^{+0.027}_{-0.027}$	$11.332^{+0.0013}_{-0.0013}$	(3.85)	$1.64^{+0.20}_{-0.18}$	Hir18	9.82 ± 0.25	493 ± 13	⋯
CD-44 170	b	$0.101^{+0.009}_{-0.013}$	$15.8190^{+0.0049}_{-0.0026}$	$>13^{+4.1}_{-6.6}$	(>3.63)	Tuo14	4.51 ± 0.35	406 ± 32	⋯
LHS 1140	b	$0.0875^{+0.0041}_{-0.0041}$	$24.73712^{+0.00025}_{-0.00025}$	$6.65^{+1.82}_{-1.82}$	$1.43^{+0.10}_{-0.10}$	Dit17	0.5780 ± 0.0072	242.7 ± 3.0	Yes
	c	$0.02675^{+0.00070}_{-0.00070}$	$3.777931^{+0.000006}_{-0.000006}$	$1.81^{+0.39}_{-0.39}$	$1.282^{+0.024}_{-0.024}$	Men19	6.184 ± 0.077	438.9 ± 5.4	⋯
2MASS J01021226-6145216	b	$0.03946^{+0.00095}_{-0.00168}$	$3.7955213^{+0.0000011}_{-0.0000011}$	(1750)	$12.106^{+0.179}_{-0.179}$	Bak18	16.18 ± 1.14	558 ± 39	⋯
BD+61 195	b	$0.0905^{+0.0011}_{-0.0011}$	$13.8508^{+0.0053}_{-0.0051}$	$>5.63^{+0.67}_{-0.68}$	(>2.25)	Per19	5.52 ± 0.12	426.7 ± 9.0	⋯
YZ Cet	b	$0.01557^{+0.00052}_{-0.00052}$	$1.96876^{+0.00021}_{-0.00021}$	$>0.75^{+0.13}_{-0.13}$	(>0.93)	Ast17a	9.08 ± 0.14	483.1 ± 7.6	⋯
	c	$0.0209^{+0.0007}_{-0.0007}$	$3.06008^{+0.00022}_{-0.00022}$	$>0.98^{+0.14}_{-0.14}$	(>1.00)	Ast17a	5.037 ± 0.079	417.0 ± 6.5	⋯
	d	$0.02764^{+0.00093}_{-0.00093}$	$4.65627^{+0.00042}_{-0.00042}$	$>1.14^{+0.17}_{-0.17}$	(>1.05)	Ast17a	2.880 ± 0.045	362.6 ± 5.7	⋯
K2-150	b	$0.0727^{+0.0027}_{-0.0027}$	$10.59357^{+0.00084}_{-0.00084}$	(5.26)	$2.00^{+0.27}_{-0.21}$	Hir18	4.24 ± 0.10	399.5 ± 9.8	⋯
K2-151	b	$0.0365^{+0.0014}_{-0.0014}$	$3.835592^{+0.000023}_{-0.000023}$	(2.44)	$1.35^{+0.16}_{-0.14}$	Hir18	24.48 ± 0.34	619.1 ± 8.7	⋯
BD-17 400	b	$0.0197^{+0.0005}_{-0.0005}$	$1.22003^{+0.00006}_{-0.00004}$	$>1.78^{+0.34}_{-0.33}$	(>1.20)	Ast17b	215.2 ± 3.4	1066 ± 17	⋯
	c	$0.057^{+0.001}_{-0.001}$	$5.974^{+0.001}_{-0.001}$	$>4.18^{+0.61}_{-0.59}$	(>1.88)	Ast17b	25.70 ± 0.41	626.7 ± 9.9	⋯
	d	$0.698^{+0.018}_{-0.019}$	$257.8^{+3.6}_{-3.5}$	$>10.5^{+2.3}_{-2.1}$	(>3.21)	Ast17b	0.1714 ± 0.0027	179.1 ± 2.8	⋯
GJ 96	b	$0.291^{+0.005}_{-0.005}$	$73.94^{+0.33}_{-0.38}$	$>19.66^{+2.20}_{-2.30}$	(>4.74)	Hob18	0.754 ± 0.011	259.4 ± 3.8	Yes
CD-23 1056	b	$0.25^{+0.01}_{-0.01}$	$53.435^{+0.042}_{-0.042}$	$>114^{+22}_{-22}$	(>13.1)	Sta17	1.45 ± 0.12	306 ± 25	Yes
LP 413-32 B	b	$0.164^{+0.03}_{-0.03}$	$31.393463^{+0.000067}_{-0.000069}$	(4.01)	$1.70^{+0.36}_{-0.36}$	Fei19	1.354 ± 0.066	300 ± 15	Yes
BD-21 784	b	$0.053^{+0.004}_{-0.007}$	$5.2354^{+0.0027}_{-0.0065}$	$>10.2^{+7.2}_{-4.1}$	(>3.10)	Tuo14	48.8 ± 2.9	736 ± 43	⋯
LPM 178	b	$0.06070^{+0.00001}_{-0.00001}$	$8.63300^{+0.00155}_{-0.00155}$	$>10.60^{+0.06}_{-0.06}$	(>3.29)	Bon13b	5.89 ± 0.10	433.6 ± 7.5	⋯
	c	$0.1254^{+0.0001}_{-0.0001}$	$25.6450^{+0.0235}_{-0.0235}$	$>6.8^{+0.9}_{-0.9}$	(>2.52)	Bon13b	1.380 ± 0.024	301.6 ± 5.2	Yes
	d	$1.0304^{+0.0086}_{-0.0086}$	$660.89^{+7.56}_{-7.56}$	$>29.4^{+2.9}_{-2.9}$	(>5.91)	Bon13b	0.02044 ± 0.00035	105.2 ± 1.8	⋯
Melotte 25 VA 50	b	$0.0299^{+0.0005}_{-0.0005}$	$3.484552^{+0.000031}_{-0.000037}$	(11.6)	$3.43^{+0.95}_{-0.31}$	Man16a	8.68 ± 0.15	477.7 ± 8.1	⋯
HG 8-15	b	$0.0562^{+0.0013}_{-0.0014}$	$6.342^{+0.002}_{-0.002}$	$4.7^{+0.5}_{-0.3}$	$1.8^{+0.2}_{-0.1}$	Die18	31.61 ± 0.49	660 ± 10	⋯
	c	$0.0946^{+0.0031}_{-0.0030}$	$13.850^{+0.006}_{-0.006}$	$6.5^{+1.5}_{-0.5}$	$2.6^{+0.7}_{-0.2}$	Die18	11.16 ± 0.17	509 ± 7.8	⋯
	d	$0.1937^{+0.0064}_{-0.0059}$	$40.718^{+0.005}_{-0.005}$	$4.9^{+1.7}_{-0.6}$	$1.9^{+0.7}_{-0.2}$	Die18	22.661 ± 0.041	355.5 ± 5.5	⋯
LP 834-042	b	$0.14339^{+0.00003}_{-0.00003}$	$30.5987^{+0.0083}_{-0.0084}$	$>23.54^{+0.88}_{-0.89}$	(>5.14)	Ast17b	1.341 ± 0.019	299.5 ± 4.2	Yes
	c	$0.36175^{+0.00048}_{-0.00047}$	$122.6196^{+0.2429}_{-0.2371}$	$>21.09^{+1.24}_{-1.26}$	(>4.88)	Ast17b	0.2108 ± 0.0030	188.6 ± 2.7	⋯
	d	$0.19394^{+0.00017}_{-0.00018}$	$48.1345^{+0.0628}_{-0.0661}$	$>7.60^{+1.05}_{-1.05}$	(>2.63)	Ast17b	0.733 ± 0.010	257.5 ± 3.7	Yes
	e	$0.08208^{+0.00003}_{-0.00004}$	$13.2543^{+0.0078}_{-0.0104}$	$>3.28^{+0.64}_{-0.64}$	(>1.62)	Ast17b	4.094 ± 0.058	395.9 ± 5.6	⋯
LEHPM 3808	b	$0.0306^{+0.0033}_{-0.0057}$	$3.360080^{+0.000065}_{-0.000070}$	(1.98)	$1.247^{+0.089}_{-0.083}$	Gun19	17.89 ± 1.44	572 ± 46	⋯
	c	$0.0472^{+0.0030}_{-0.0033}$	$5.660172^{+0.000035}_{-0.000035}$	(6.88)	$2.42^{+0.13}_{-0.13}$	Gun19	7.52 ± 0.14	460.9 ± 8.3	⋯
	d	$0.0733^{+0.0042}_{-0.0042}$	$11.38014^{+0.00011}_{-0.00010}$	(5.48)	$2.13^{+0.12}_{-0.12}$	Gun19	3.119 ± 0.052	369.9 ± 6.2	⋯
LP 358-499	b	$0.033^{+0.002}_{-0.002}$	$3.0712^{+0.0001}_{-0.0001}$	(2.29)	$1.31^{+0.08}_{-0.08}$	Wel17	32.26 ± 0.39	663.3 ± 8.0	⋯
	c	$0.045^{+0.003}_{-0.003}$	$4.8682^{+0.0001}_{-0.0003}$	(3.07)	$1.48^{+0.09}_{-0.09}$	Wel17	17.35 ± 0.21	568.0 ± 6.8	⋯
	d	$0.077^{+0.005}_{-0.005}$	$11.0234^{+0.0008}_{-0.0003}$	(5.15)	$2.02^{+0.13}_{-0.13}$	Wel17	5.925 ± 0.071	434.2 ± 5.2	⋯
HD 285968	b	$0.066^{+0.001}_{-0.001}$	$8.776^{+0.001}_{-0.002}$	$>9.06^{+1.54}_{-0.70}$	(>2.87)	Tri18	8.37 ± 0.17	473.5 ± 9.5	⋯
Wolf 1539	b	$2.41^{+0.04}_{-0.04}$	2288^{+59}_{-59}	$>260.61^{+22.25}_{-22.25}$	(>13.9)	How10	0.002714 ± 0.000052	63.5 ± 1.2	⋯
LPM 198	b	$0.103^{+0.006}_{-0.014}$	$17.380^{+0.018}_{-0.020}$	$>8.3^{+3.5}_{-5.3}$	(>2.81)	Tuo14	2.29 ± 0.18	342.3 ± 27.1	Yes
	c	$0.1290^{+0.0070}_{-0.0017}$	$24.329^{+0.052}_{-0.066}$	$>6.4^{+3.7}_{-4.1}$	(>2.43)	Tuo14	1.459 ± 0.064	306 ± 13	⋯
LP 656-38	b	$0.03282^{+0.00054}_{-0.00056}$	$5.3636^{+0.0007}_{-0.0007}$	$>2.02^{+0.26}_{-0.25}$	(>1.23)	Ast17b	3.392 ± 0.049	377.7 ± 5.5	⋯
	c	$0.1264^{+0.0021}_{-0.0022}$	$40.54^{+0.21}_{-0.19}$	$>2.31^{+0.50}_{-0.49}$	(>1.32)	Ast17b	0.2287 ± 0.0033	192.5 ± 2.8	⋯
Kapteyn's	b	$0.168^{+0.006}_{-0.008}$	$48.616^{+0.036}_{-0.036}$	$>4.8^{+0.9}_{-1.0}$	(>1.98)	Ang14	0.454 ± 0.014	228.4 ± 6.9	Yes
	c	$0.311^{+0.038}_{-0.014}$	$121.54^{+0.25}_{-0.25}$	$>7.0^{+1.2}_{-1.0}$	(>2.54)	Ang14	0.132 ± 0.012	167.9 ± 13.8	⋯
LP 892-26	b	0.089	$14.207^{+0.007}_{-0.007}$	$>6.60^{+0.01}_{-0.01}$	(>2.43)	Ast15	4.1	395	⋯
NGTS-1	b	$0.0326^{+0.0047}_{-0.0045}$	$2.647298^{+0.000020}_{-0.000020}$	$258.1^{+20.9}_{-23.8}$	$14.91^{+6.84}_{-3.70}$	Bay18	63.9 ± 1.4	786.8 ± 16.9	⋯
HATS-6	b	$0.03623^{+0.00042}_{-0.00057}$	$3.3252725^{+0.0000021}_{-0.0000021}$	$101.4^{+22.2}_{-22.2}$	$11.19^{+0.21}_{-0.21}$	Har15	53.5 ± 1.2	752.7 ± 16.8	⋯
BD-06 1339	b	$0.0428^{+0.0007}_{-0.0007}$	$3.8728^{+0.0004}_{-0.0004}$	$>8.5^{+1.3}_{-1.3}$	(>2.81)	LoC13	56.7 ± 1.3	763.9 ± 17.8	⋯
	c	$0.457^{+0.007}_{-0.007}$	$125.95^{+0.44}_{-0.44}$	$>53^{+8}_{-8}$	(>8.42)	LoC13	0.498 ± 0.012	233.8 ± 5.4	Yes

Table 6
(Continued)

Name	Planet	a (au)	P_{orb} (days)	M_p[a] ($M_\oplus$)	R_p[a] ($R_\oplus$)	References[b]	S_{eff} ($S_\odot$)	$T_{eq,p}$ (K)	Potentially HZ
HD 42581	b	$0.97^{+0.12}_{-0.09}$	471^{+22}_{-12}	$>32^{+17}_{-16}$	(>6.21)	Tuo14	0.0576 ± 0.0035	136.3 ± 8.3	⋯
PM J06168+2435	b	$0.0962^{+0.0054}_{-0.0061}$	$14.5665^{+0.0016}_{-0.0020}$	(7.64)	$2.67^{+0.46}_{-0.42}$	Sch16	4.79 ± 0.10	411.8 ± 8.9	⋯
Luyten's star	b	$0.091101^{+0.000019}_{-0.000017}$	$18.6498^{+0.0059}_{-0.0052}$	$>2.89^{+0.27}_{-0.26}$	(>1.45)	Ast17b	1.193 ± 0.042	291 ± 10	Yes
	c	$0.036467^{+0.000002}_{-0.000002}$	$4.7234^{+0.0004}_{-0.0004}$	$>1.18^{+0.16}_{-0.16}$	(>1.06)	Ast17b	7.44 ± 0.26	460 ± 16	⋯
LP 424-4	b	$0.0348^{+0.0014}_{-0.0014}$	$3.33714^{+0.00017}_{-0.00017}$	$14.0^{+1.7}_{-1.7}$	$4.2^{+0.6}_{-0.6}$	Bon12	33.07 ± 0.41	667.4 ± 8.2	⋯
NGC 2632 JS 183	b	$0.0653^{+0.0039}_{-0.0045}$	$10.13389^{+0.00068}_{-0.00077}$	$0.361^{+0.069}_{-0.069}$	$3.47^{+0.78}_{-0.53}$	Obe16	5.13 ± 0.27	419 ± 22	⋯
K2-146	b	$0.0266^{+0.0010}_{-0.0010}$	$2.644646^{+0.000043}_{-0.000043}$	(5.48)	$2.2^{+0.23}_{-0.23}$	Hir18	17.47 ± 0.38	569 ± 13	⋯
LP 844-8	b	$1.15^{+0.05}_{-0.05}$	692^{+2}_{-2}	$>572.07^{+15.89}_{-15.89}$	(>13.3)	Ang12	0.01695 ± 0.00029	100.4 ± 8.9	⋯
	c	5.5	7100^{+8000}_{-1500}	509	(>13.5)	Ang12	0.00074	46	⋯
NGC 2632 JS 597	b	$0.05023^{+0.00042}_{-0.00043}$	$5.840002^{+0.000676}_{-0.000602}$	(5.83)	$2.231^{+0.151}_{-0.145}$	Liv19	12.57 ± 0.38	524 ± 16	⋯
	c	$0.11283^{+0.00095}_{-0.00097}$	$19.660302^{+0.003496}_{-0.003337}$	(7.64)	$2.668^{+0.201}_{-0.194}$	Liv19	2.490 ± 0.075	350 ± 11	⋯
BD+02 2098	b	$4.5^{+0.2}_{-0.2}$	4100^{+300}_{-300}	$>2.30^{+0.13}_{-0.13}$	(>1.32)	Rob13	0.004911 ± 0.000060	73.68 ± 0.90	⋯
K2-117	b	$0.019^{+0.001}_{-0.001}$	$1.291505^{+0.000040}_{-0.000040}$	(4.84)	$1.96^{+0.12}_{-0.12}$	Dre17	123.1 ± 2.6	927 ± 20	⋯
	c	$0.051^{+0.002}_{-0.002}$	$5.444820^{+0.000397}_{-0.000417}$	(5.26)	$2.03^{+0.13}_{-0.13}$	Dre17	17.09 ± 0.36	565 ± 12	⋯
BD+48 1829	b	$0.039435^{+0.00023}_{-0.00023}$	$3.822^{+0.001}_{-0.001}$	$>13.02^{+2.03}_{-2.01}$	(>3.62)	Hob19	37.08 ± 0.67	687 ± 13	⋯
LTT 3758	b	$0.0153^{+0.0005}_{-0.0005}$	$1.628931^{+0.000027}_{-0.000027}$	$1.66^{+0.23}_{-0.23}$	$1.43^{+0.16}_{-0.16}$	Sou17, Bon18b	19.88 ± 0.25	587.7 ± 7.3	⋯
	c	$0.0476^{+0.0017}_{-0.0017}$	$8.929^{+0.010}_{-0.010}$	$>2.64^{+0.44}_{-0.44}$	(>1.40)	Bon18b	2.054 ± 0.026	333.2 ± 4.2	⋯
K2-239	b	$0.0441^{+0.0008}_{-0.0008}$	$5.240^{+0.001}_{-0.001}$	$1.4^{+0.4}_{-0.4}$	$1.1^{+0.1}_{-0.1}$	Die18	3.697 ± 0.048	385.9 ± 5.0	⋯
	c	$0.0576^{+0.0009}_{-0.0009}$	$7.775^{+0.001}_{-0.001}$	$0.9^{+0.3}_{-0.3}$	$1.1^{+0.1}_{-0.1}$	Die18	2.167 ± 0.026	337.7 ± 4.4	⋯
	d	$0.0685^{+0.0012}_{-0.0012}$	$10.115^{+0.001}_{-0.001}$	$1.3^{+0.4}_{-0.4}$	$1.1^{+0.1}_{-0.1}$	Die18	1.532 ± 0.048	309.7 ± 4.0	⋯
LP 905-36	b	$0.0287^{+0.0010}_{-0.0011}$	$2.64561^{+0.00066}_{-0.00066}$	$7.0^{+0.9}_{-0.8}$[c]	(>2.54)	Bon11	35.02 ± 0.56	677.0 ± 10.7	⋯
Lalande 21185	b	0.0695	$9.8693^{+0.0016}_{-0.0016}$	3.8	(>1.75)	But17	3.84 ± 0.27	390 ± 27	⋯
Innes' star	b	$0.119^{+0.014}_{-0.009}$	$26.161^{+0.082}_{-0.098}$	$>9.9^{+5.6}_{-4.0}$	(>3.13)	Tuo14	1.264 ± 0.056	295 ± 13	Yes
K2-22	b	0.009	$0.381078^{+0.000003}_{-0.000003}$	(20.2)	$4.75^{+0.35}_{-0.36}$	Dre17	1000	1565	⋯
PM J11293-0127	b	$0.0769^{+0.0039}_{-0.0039}$	$10.05449^{+0.00026}_{-0.00026}$	$8.4^{+2.1}_{-2.1}$	$2.18^{+0.3}_{-0.3}$	Alm15, Sin16	10.20 ± 0.20	497.4 ± 9.9	⋯
	c	$0.1399^{+0.0070}_{-0.0070}$	$24.64354^{+0.00117}_{-0.00117}$	$2.1^{+2.1}_{-1.3}$	$1.85^{+0.27}_{-0.27}$	Alm15, Sin16	3.083 ± 0.062	368.8 ± 7.4	⋯
	d	$0.2076^{+0.0104}_{-0.0104}$	$44.55983^{+0.00590}_{-0.00590}$	$11.1^{+3.5}_{-3.5}$	$1.51^{+0.23}_{-0.23}$	Alm15, Sin16	1.400 ± 0.028	302.8 ± 6.0	Yes
PM J11302+0735	b	$0.1429^{+0.0060}_{-0.0065}$	$32.939614^{+0.000101}_{-0.000084}$	$8.43^{+1.44}_{-1.35}$	$2.38^{+0.22}_{-0.22}$	Clo17, Sar18	1.293 ± 0.021	296.8 ± 4.8	Yes
	c	$0.060^{+0.003}_{-0.003}$	$8.962^{+0.008}_{-0.008}$	$>7.51^{+1.33}_{-1.33}$	(>2.66)	Clo17	7.33 ± 0.12	458.0 ± 7.3	⋯
CD-31 9113	b	$0.060^{+0.004}_{-0.008}$	$7.3697^{+0.0034}_{-0.0036}$	$>5.3^{+2.0}_{-1.9}$	(>2.19)	Tuo14	9.43 ± 0.65	487.7 ± 33.4	⋯
	c	3.6	3693^{+253}_{-253}	44.6	(> 7.73)	Del13	0.0026	63	⋯
Ross 1003	b	$0.166^{+0.001}_{-0.001}$	$41.380^{+0.002}_{-0.001}$	$>96.70^{+1.41}_{-1.02}$	(>11.9)	Tri18	0.5440 ± 0.0061	239.0 ± 2.7	Yes
	c	$0.912^{+0.005}_{-0.002}$	$532.58^{+4.14}_{-2.52}$	$>68.06^{+4.91}_{-2.19}$	(>9.40)	Tri18	0.01802 ± 0.00021	102.0 ± 1.2	⋯
Ross 905	b	$0.028^{+0.001}_{-0.001}$	$2.644^{+0.001}_{-0.001}$	$>21.36^{+0.20}_{-0.21}$	$4.170^{+0.168}_{-0.168}$	Mac14, Tri18	30.48 ± 0.45	653.9 ± 9.7	⋯
LP 613-39	b	$0.0910^{+0.0130}_{-0.0160}$	$18.4498^{+0.0015}_{-0.0015}$	(5.83)	$2.25^{+0.53}_{-0.96}$	Sch16	1.470 ± 0.054	306.4 ± 11.3	Yes
FI Vir	b	$0.0496^{+0.0017}_{-0.0017}$	$9.8658^{+0.0070}_{-0.0070}$	$>1.4^{+0.21}_{-0.21}$	(>1.11)	Bon18b	1.556 ± 0.023	310.8 ± 4.5	⋯
K2-152	b	$0.1735^{+0.0054}_{-0.0054}$	$32.6527^{+0.0035}_{-0.0035}$	(8.30)	$2.81^{+0.34}_{-0.30}$	Hir18	2.944 ± 0.054	364.6 ± 6.6	⋯
K2-153	b	$0.0601^{+0.0021}_{-0.0021}$	$7.51554^{+0.00098}_{-0.00098}$	(4.89)	$2.00^{+0.26}_{-0.22}$	Hir18	14.82 ± 0.33	546 ± 12	⋯
K2-137	b	$0.0058^{+0.0006}_{-0.0006}$	$0.179715^{+0.000006}_{-0.000006}$	(0.65)	$0.89^{+0.09}_{-0.09}$	Smi18	841 ± 18	1499 ± 33	⋯
K2-154	b	$0.0408^{+0.0012}_{-0.0012}$	$3.67635^{+0.00017}_{-0.00017}$	(6.08)	$2.23^{+0.37}_{-0.24}$	Hir18	59.04 ± 0.96	772 ± 13	⋯
	c	$0.0683^{+0.0021}_{-0.0021}$	$7.95478^{+0.00063}_{-0.00063}$	(5.48)	$2.10^{+0.25}_{-0.23}$	Hir18	21.07 ± 0.34	596.3 ± 9.7	⋯
Ross 1020	b	$0.026^{+0.001}_{-0.001}$	$3.023^{+0.001}_{-0.001}$	$>7.0^{+0.5}_{-0.5}$	(>2.54)	Luq18	12.16 ± 0.16	519.7 ± 6.6	⋯
HD 122303	b	$0.067^{+0.001}_{-0.001}$	$8.708^{+0.002}_{-0.001}$	$>6.51^{+0.69}_{-0.40}$	(>2.42)	Tri18	9.66 ± 0.16	490.6 ± 8.2	⋯
Proxima Cen	b	$0.0485^{+0.0041}_{-0.0041}$	$11.186^{+0.001}_{-0.001}$	$>1.27^{+0.19}_{-0.17}$	(>1.07)	Ang16	0.653 ± 0.017	250.2 ± 6.4	Yes
K2-240	b	$0.0513^{+0.0009}_{-0.0009}$	$6.034^{+0.001}_{-0.001}$	$5.0^{+0.5}_{-0.2}$	$2.0^{+0.2}_{-0.1}$	Die18	23.88 ± 0.58	615 ± 15	⋯
	c	$0.1159^{+0.0020}_{-0.0020}$	$20.523^{+0.001}_{-0.001}$	$4.6^{+0.7}_{-0.3}$	$1.8^{+0.3}_{-0.1}$	Die18	4.68 ± 0.11	409 ± 10	⋯
HO Lib	b	$0.041^{+0.001}_{-0.001}$	$5.368^{+0.001}_{-0.001}$	$>15.20^{+0.22}_{-0.27}$	(>4.03)	Tri18	7.14 ± 0.10	455.0 ± 6.4	⋯
	c	$0.074^{+0.001}_{-0.001}$	$12.919^{+0.003}_{-0.002}$	$> 5.652^{+0.386}_{-0.239}$	(>2.20)	Tri18	2.192 ± 0.031	338.6 ± 4.7	⋯
	d	$0.029^{+0.001}_{-0.001}$	$3.153^{+0.001}_{-0.006}$	$>1.657^{+0.240}_{-0.161}$	(>1.18)	Tri18	14.27 ± 0.20	541.0 ± 7.6	⋯

Table 6
(Continued)

Name	Planet	a (au)	P_{orb} (days)	M_p[a] ($M_\oplus$)	R_p[a] ($R_\oplus$)	References[b]	S_{eff} ($S_\odot$)	$T_{eq,p}$ (K)	Potentially HZ
K2-286	b	$0.1768^{+0.0175}_{-0.0205}$	$27.359^{+0.005}_{-0.005}$	(5.26)	$2.1^{+0.2}_{-0.2}$	Die19	2.891 ± 0.063	362.9 ± 7.9	…
MCC 759	b	$0.0608^{+0.0068}_{-0.0068}$	$6.905^{+0.040}_{-0.040}$	$>7.14^{+0.59}_{-0.59}$	(>2.67)	Per17	17.5 ± 0.2	569.1 ± 6.4	…
USco J161014.7-191909	b	$0.0409^{+0.0021}_{-0.0023}$	$5.424865^{+0.000035}_{-0.000031}$	<11.76	$5.04^{+0.34}_{-0.37}$	Dav16, Man16b	60.9 ± 1.9	778 ± 25	…
LP 804-27	b	0.36	$111.7^{+0.7}_{-0.7}$	>667.415	(>13.2)	App10	0.23	193	…
HD 147379	b	$0.3193^{+0.0002}_{-0.0002}$	$86.54^{+0.07}_{-0.06}$	$>24.7^{+1.8}_{-2.4}$	(>5.28)	Rei18	0.959 ± 0.023	275.4 ± 6.5	Yes
MCC 767	b	$0.078361^{+0.000044}_{-0.000046}$	$14.628^{+0.012}_{-0.013}$	$>2.82^{+0.51}_{-0.51}$	(>1.45)	Sua17	2.412 ± 0.033	346.8 ± 4.8	…
V2306 Oph	b	$0.0375^{+0.0012}_{-0.0013}$	$4.8869^{+0.0005}_{-0.0005}$	$>1.91^{+0.26}_{-0.25}$	(>1.23)	Ast17b	7.70 ± 0.12	463.6 ± 7.1	…
	c	$0.0890^{+0.0029}_{-0.0031}$	$17.8719^{+0.0059}_{-0.0059}$	$>3.41^{+0.43}_{-0.41}$	(>1.66)	Ast17b	1.366 ± 0.021	300.9 ± 4.6	Yes
	d	$0.470^{+0.015}_{-0.017}$	$217.21^{+0.55}_{-0.52}$	$>7.70^{+1.12}_{-1.06}$	(>2.66)	Ast17b	0.04899 ± 0.00077	130.9 ± 2.1	…
BD+25 3173	b	$1.135^{+0.035}_{-0.035}$	$598.3^{+4.2}_{-4.2}$	$>104.244^{+10.170}_{-10.170}$	(>12.5)	Jon10	0.03372 ± 0.00036	119.3 ± 1.3	…
LHS 3275	b	$0.01411^{+0.00032}_{-0.00032}$	$1.58040456^{+0.00000016}_{-0.00000016}$	$6.55^{+0.98}_{-0.98}$	$2.85^{+0.20}_{-0.20}$	Cha09, Har13	19.51 ± 0.25	584.9 ± 7.6	…
BD+11 3149	b	$0.029^{+0.001}_{-0.001}$	$2.64977^{+0.00081}_{-0.00077}$	$>2.47^{+0.27}_{-0.27}$	(>1.36)	Aff16	55.6 ± 1.5	760 ± 20	…
	c	$0.089^{+0.003}_{-0.003}$	$13.740^{+0.016}_{-0.016}$	$>6.26^{+0.79}_{-0.76}$	(>2.36)	Aff16	5.90 ± 0.16	434 ± 11	…
HD 156384C	b	$0.0505^{+0.0053}_{-0.0044}$	$7.2004^{+0.0017}_{-0.0017}$	$>5.6^{+1.4}_{-1.3}$	(>2.23)	Ang13	5.86 ± 0.14	433 ± 10	…
	c	$0.125^{+0.012}_{-0.013}$	$28.14^{+0.03}_{-0.03}$	$>3.8^{+1.5}_{-1.2}$	(>1.78)	Ang13	0.956 ± 0.016	275.2 ± 4.7	Yes
	d	$0.276^{+0.024}_{-0.030}$	$91.61^{+0.81}_{-0.89}$	$>5.1^{+1.8}_{-1.7}$	(>2.08)	Ang13	0.1962 ± 0.0052	185.2 ± 4.9	…
	e	$0.213^{+0.020}_{-0.020}$	$62.24^{+0.55}_{-0.55}$	$>2.7^{+1.6}_{-1.4}$	(>1.47)	Ang13	0.3294 ± 0.0050	210.9 ± 3.2	Yes
	f	$0.156^{+0.014}_{-0.017}$	$39.026^{+0.194}_{-0.211}$	$>2.7^{+1.4}_{-1.2}$	(>1.42)	Ang13	0.614 ± 0.015	246.4 ± 6.0	Yes
	g	$0.549^{+0.052}_{-0.058}$	$256.2^{+13.8}_{-7.9}$	$>4.6^{+2.6}_{-2.3}$	(>1.98)	Ang13	0.04958 ± 0.00092	131.3 ± 2.4	…
CD-46 11540	b	0.039	$4.6938^{+0.0070}_{-0.0070}$	>11.09	(>3.32)	Bon07	11	507	…
CD-51 10924	b	$1.8049^{+0.0302}_{-0.0302}$	$1051.1^{+0.5}_{-0.5}$	$>1497.9^{+2.9}_{-2.9}$	(>12.8)	Sah16	0.02763 ± 0.00050	113.5 ± 2.0	…
	c	$6.6675^{+0.4684}_{-0.4684}$	$7462.9^{+105.4}_{-101.4}$	$>2190^{+32}_{-32}$	(>12.6)	Sah16	0.002024 ± 0.000037	59.0 ± 1.1	…
	d	$0.0410^{+0.0007}_{-0.0007}$	$3.6005^{+0.0002}_{-0.0002}$	$>4.4^{+0.3}_{-0.3}$	(>1.94)	Sah16	53.50 ± 0.96	753 ± 14	…
	e	$0.1882^{+0.0032}_{-0.0032}$	$35.39^{+0.03}_{-0.04}$	$>8.1^{+0.7}_{-0.7}$	(>2.71)	Sah16	2.541 ± 0.046	351.4 ± 6.3	…
BD+68 946	b	$0.71^{+0.01}_{-0.01}$	$38.140^{+0.015}_{-0.015}$	$>19^{+3}_{-3}$	(>4.57)	Sta17	0.0439 ± 0.0010	127.4 ± 2.8	…
CD-44 11909	b	$0.08^{+0.014}_{-0.004}$	$17.478^{+0.062}_{-0.040}$	$>4.4^{+3.7}_{-2.4}$	(>1.92)	Tuo14	1.268 ± 0.159	295 ± 37	Yes
	c	$0.176^{+0.030}_{-0.009}$	$57.32^{+0.45}_{-0.48}$	$>8.7^{+5.8}_{-4.6}$	(>2.81)	Tuo14	0.262 ± 0.031	199 ± 24	Yes
BD+18 3421	b	$0.091^{+0.004}_{-0.004}$	$15.53209^{+0.00166}_{-0.00167}$	$>7.1^{+0.9}_{-0.9}$	(>2.58)	Aff19	3.34 ± 0.22	376 ± 25	…
Barnard's star	b	$0.404^{+0.018}_{-0.018}$	$232.80^{+0.38}_{-0.41}$	$>3.23^{+0.44}_{-0.44}$	(>1.58)	Rib18	0.02180 ± 0.00044	106.9 ± 2.2	…
Kepler-83	b	0.0785	$9.770469^{+0.000022}_{-0.000022}$	(7.03)	$2.53^{+0.16}_{-0.16}$	Row14	15	547	…
	c	0.0514	$5.169796^{+0.000016}_{-0.000016}$	(4.74)	$1.94^{+0.13}_{-0.13}$	Row14	35	676	…
	d	0.1270	$20.090227^{+0.000102}_{-0.000102}$	(6.08)	$2.30^{+0.35}_{-0.35}$	Row14	5.7	430	…
Kepler-446	b	$0.0159^{+0.0007}_{-0.0007}$	$1.5654090^{+0.0000033}_{-0.0000033}$	$4.5^{+0.5}_{-0.5}$	$1.50^{+0.25}_{-0.25}$	Mui15	19.61 ± 0.39	586 ± 12	…
	c	$0.0248^{+0.0011}_{-0.0011}$	$3.0361790^{+0.0000055}_{-0.0000055}$	3^{+1}_{-1}	$1.11^{+0.18}_{-0.18}$	Mui15	8.11 ± 0.16	469.6 ± 9.3	…
	d	$0.0352^{+0.0016}_{-0.0016}$	$5.148921^{+0.000022}_{-0.000022}$	4^{+1}_{-1}	$1.35^{+0.22}_{-0.22}$	Mui15	4.008 ± 0.079	393.8 ± 7.8	…
Kepler-303	b	0.0265	$1.937055^{+0.000004}_{-0.000004}$	(0.66)	$0.89^{+0.05}_{-0.05}$	Row14	125	930	…
	c	0.0628	$7.061149^{+0.000019}_{-0.000019}$	(1.55)	$1.14^{+0.09}_{-0.09}$	Row14	22	604	…
Kepler-617	b	0.0233	$1.682696148^{+0.000001112}_{-0.000001112}$	(2.32)	$1.32^{+0.07}_{-0.07}$	Mor16	94	867	…
Kepler-236	b	0.0698	$8.295611^{+0.000032}_{-0.000032}$	(3.40)	$1.57^{+0.12}_{-0.12}$	Row14	15	552	…
	c	0.1416	$23.968127^{+0.000174}_{-0.000174}$	(4.94)	$2.00^{+0.17}_{-0.17}$	Row14	3.8	388	…
Kepler-235	b	0.035	$3.340222^{+0.000005}_{-0.000005}$	(5.83)	$2.23^{+0.10}_{-0.10}$	Row14	71	810	…
	c	0.037	$7.824904^{+0.000055}_{-0.000055}$	(2.02)	$1.28^{+0.08}_{-0.08}$	Row14	64	788	…
	d	0.122	$20.060548^{+0.000099}_{-0.000099}$	(5.26)	$2.05^{+0.10}_{-0.10}$	Row14	5.9	434	…
	e	0.213	$46.183669^{+0.000425}_{-0.000425}$	(5.95)	$2.22^{+0.29}_{-0.29}$	Row14	1.9	328	…
Kepler-52	b	…	$7.877407^{+0.000020}_{-0.000020}$	(6.08)	$2.34^{+0.22}_{-0.22}$	Row14	22	604	…
	c	…	$16.384888^{+0.000080}_{-0.000080}$	(4.01)	$1.71^{+0.08}_{-0.08}$	Row14	8.4	474	…
	d	…	$36.445171^{+0.000253}_{-0.000253}$	(4.74)	$1.95^{+0.21}_{-0.21}$	Row14	2.9	363	…
Kepler-155	b	0.056	$5.931194^{+0.000008}_{-0.000008}$	(5.26)	$2.09^{+0.21}_{-0.21}$	Row14	55	758	…
	c	0.242	$52.661793^{+0.000236}_{-0.000236}$	(5.83)	$2.24^{+0.15}_{-0.15}$	Row14	2.9	365	…

Table 6
(Continued)

Name	Planet	a (au)	P_{orb} (days)	M_p[a] ($M_\oplus$)	R_p[a] ($R_\oplus$)	References[b]	S_{eff} ($S_\odot$)	$T_{eq,p}$ (K)	Potentially HZ
V1428 Aql	b	$0.3357^{+0.0099}_{-0.0100}$	$105.90^{+0.09}_{-0.10}$	$>12.2^{+1.0}_{-1.4}$	(>3.40)	Kam18	0.2891 ± 0.0035	204.1 ± 2.5	Yes
Kepler-138	b	$0.0746^{+0.0021}_{-0.0021}$	$10.3126^{+0.0004}_{-0.0006}$	$0.066^{+0.059}_{-0.037}$	$0.522^{+0.032}_{-0.032}$	Jhu15	10.34 ± 0.14	499.1 ± 6.5	⋯
	c	$0.0905^{+0.0026}_{-0.0026}$	$13.7813^{+0.0001}_{-0.0001}$	$1.970^{+1.912}_{-1.120}$	$1.197^{+0.070}_{-0.070}$	Jhu15	7.026 ± 0.092	453.1 ± 5.9	⋯
	d	$0.1277^{+0.0036}_{-0.0036}$	$23.0881^{+0.0009}_{-0.0008}$	$0.640^{+0.674}_{-0.387}$	$2.1^{+2.2}_{-1.2}$	Jhu15	3.531 ± 0.046	381.5 ± 5.0	⋯
LSPM J1928+4437	b	0.0116	$1.2137672^{+0.0000046}_{-0.0000046}$	(0.39)	$0.78^{+0.22}_{-0.22}$	Mui12b	22	600	⋯
	c	0.006	$0.45328509^{+0.00000097}_{-0.00000097}$	(0.33)	$0.73^{+0.20}_{-0.20}$	Mui12b	81	834	⋯
	d	0.0154	$1.865169^{+0.000014}_{-0.000014}$	(0.13)	$0.57^{+0.18}_{-0.18}$	Mui12b	12	521	⋯
Kepler-49	b	0.0642	$7.203871^{+0.000008}_{-0.000008}$	(6.21)	$2.35^{+0.09}_{-0.09}$	Row14	23	609	⋯
	c	0.0847	$10.912732^{+0.000021}_{-0.000021}$	(5.10)	$2.06^{+0.09}_{-0.09}$	Row14	13	530	⋯
	d	0.0323	$2.576549^{+0.000003}_{-0.000003}$	(3.55)	$1.60^{+0.07}_{-0.07}$	Row14	90	858	⋯
	e	0.1208	$18.596108^{+0.000079}_{-0.000079}$	(3.33)	$1.56^{+0.08}_{-0.08}$	Row14	6.5	444	⋯
LSPM J1930+4149	b	$0.0514^{+0.0028}_{-0.0028}$	$8.689090^{+0.000024}_{-0.000024}$	(1.28)	$1.08^{+0.15}_{-0.15}$	Age17	1.982 ± 0.039	330.2 ± 6.6	⋯
Kepler-45	b	0.03	$2.455239^{+0.000004}_{-0.000004}$	$160.497^{+28.604}_{-28.604}$	$10.76^{+1.23}_{-1.23}$	Jon12	90	856	⋯
Kepler-231	b	0.0788	$10.065275^{+0.000027}_{-0.000027}$	(4.10)	$1.73^{+0.12}_{-0.12}$	Row14	13	530	⋯
	c	0.1215	$19.271566^{+0.000099}_{-0.000099}$	(4.74)	$1.93^{+0.19}_{-0.19}$	Row14	5.5	427	⋯
Kepler-54	b	0.0655	$8.010260^{+0.000030}_{-0.000030}$	(5.15)	$2.07^{+0.12}_{-0.12}$	Row14	11	509	⋯
	c	0.0862	$12.072389^{+0.000100}_{-0.000100}$	(4.23)	$1.75^{+0.12}_{-0.12}$	Row14	6.5	444	⋯
	d	0.1246	$20.995694^{+0.000143}_{-0.000143}$	(3.26)	$1.53^{+0.08}_{-0.08}$	Row14	3.1	369	⋯
Kepler-252	b	0.0631	$6.668391^{+0.000031}_{-0.000031}$	(1.90)	$1.23^{+0.12}_{-0.12}$	Row14	36	680	⋯
	c	0.0873	$10.848463^{+0.000015}_{-0.000015}$	(5.37)	$2.15^{+0.13}_{-0.13}$	Row14	19	578	⋯
Kepler-32	b	0.05	$5.90124^{+0.00010}_{-0.00010}$	(5.89)	$2.2^{+0.2}_{-0.2}$	Fab12	26	629	⋯
	c	0.09	$8.7522^{+0.0003}_{-0.0003}$	(4.94)	$2.0^{+0.2}_{-0.2}$	Fab12	8.0	469	⋯
	d	0.13	$22.7802^{+0.0005}_{-0.0005}$	(7.96)	$2.7^{+0.2}_{-0.2}$	Fab12	3.9	390	⋯
	e	0.033	$2.8960^{+0.0003}_{-0.0003}$	(4.36)	$1.85^{+0.01}_{-0.01}$	Fab12	60	7734	⋯
	f	0.013	$0.74296^{+0.00007}_{-0.00007}$	(0.47)	$0.82^{+0.07}_{-0.07}$	Fab12	385	1233	⋯
Kepler-125	b	0.0427	$4.164389^{+0.000003}_{-0.000003}$	(6.34)	$2.37^{+0.10}_{-0.10}$	Row14	31	655	⋯
	c	0.0531	$5.774464^{+0.000047}_{-0.000047}$	(0.32)	$0.74^{+0.05}_{-0.05}$	Row14	20	587	⋯
Kepler-186	b	$0.0343^{+0.0046}_{-0.0046}$	$3.8867907^{+0.0000062}_{-0.0000063}$	(1.21)	$1.07^{+0.12}_{-0.12}$	Qui14	48.6 ± 1.2	735 ± 19	⋯
	c	$0.0451^{+0.0070}_{-0.0070}$	$7.267302^{+0.000012}_{-0.000011}$	(2.02)	$1.25^{+0.14}_{-0.14}$	Qui14	28.09 ± 0.71	641 ± 16	⋯
	d	$0.0781^{+0.0100}_{-0.0100}$	$13.342996^{+0.000025}_{-0.000024}$	(2.65)	$1.40^{+0.16}_{-0.16}$	Qui14	9.37 ± 0.24	487 ± 12	⋯
	e	$0.110^{+0.015}_{-0.015}$	$22.407704^{+0.000074}_{-0.000072}$	(2.05)	$1.27^{+0.15}_{-0.14}$	Qui14	4.72 ± 0.12	410 ± 10	⋯
	f	$0.432^{+0.171}_{-0.053}$	$129.9441^{+0.0013}_{-0.0012}$	(1.65)	$1.17^{+0.08}_{-0.08}$	Tor15	0.306 ± 0.084	207 ± 57	Yes
Kepler-445	b	$0.0229^{+0.0010}_{-0.0010}$	$2.984151^{+0.000011}_{-0.000011}$	(3.55)	$1.58^{+0.23}_{-0.23}$	Mui15	14.79 ± 0.40	546 ± 15	⋯
	c	$0.0318^{+0.0013}_{-0.0013}$	$4.871229^{+0.000011}_{-0.000011}$	(6.74)	$2.51^{+0.36}_{-0.36}$	Mui15	7.70 ± 0.21	464 ± 13	⋯
	d	$0.0448^{+0.0019}_{-0.0019}$	$8.15275^{+0.00040}_{-0.00040}$	(1.86)	$1.25^{+0.19}_{-0.19}$	Mui15	3.87 ± 0.11	390 ± 11	⋯
Kepler-267	b	0.0370	$3.353728^{+0.000007}_{-0.000007}$	(5.04)	$1.98^{+0.09}_{-0.09}$	Row14	43	712	⋯
	c	0.0597	$6.877450^{+0.000016}_{-0.000016}$	(5.59)	$2.13^{+0.11}_{-0.11}$	Row14	16	560	⋯
	d	0.1539	$28.464515^{+0.000180}_{-0.000180}$	(5.71)	$2.27^{+0.12}_{-0.12}$	Row14	2.5	349	⋯
HD 204961	b	$3.56^{+0.28}_{-0.28}$	3657^{+104}_{-104}	$>216^{+29}_{-28}$	(>13.8)	Wit14	0.002304 ± 0.000088	61.0 ± 2.3	⋯
	c	$0.163^{+0.006}_{-0.006}$	$35.68^{+0.03}_{-0.03}$	$>5.40^{+0.95}_{-0.95}$	(>2.16)	Wit14	1.099 ± 0.042	285 ± 11	Yes
BD-05 5715	b	$2.35^{+0.22}_{-0.22}$	1882^{+250}_{-250}	$>318^{+99}_{-99}$	(>13.5)	Sta17	0.005115 ± 0.000077	74.4 ± 1.1	⋯
	c	6.5640	8775	>245.7	(>13.9)	Mon14	0.00066	45	⋯
LP 819-052	b	$0.026^{+0.001}_{-0.001}$	$3.651^{+0.001}_{-0.001}$	$>6.4^{+0.5}_{-0.5}$	(>2.36)	Luq18	5.378 ± 0.068	423.8 ± 5.4	⋯
LP 700-6	b	$0.0214^{+0.0013}_{-0.0013}$	$2.260455^{+0.000041}_{-0.000041}$	(6.08)	$2.32^{+0.24}_{-0.24}$	Hir16	25.50 ± 0.50	625 ± 12	⋯
K2-21	b	$0.076^{+0.002}_{-0.003}$	$9.325038^{+0.000379}_{-0.000403}$	(4.45)	$1.84^{+0.10}_{-0.10}$	Dre17	16.93 ± 0.32	565 ± 11	⋯
	c	$0.107^{+0.003}_{-0.004}$	$15.50192^{+0.00092}_{-0.00093}$	(7.18)	$2.49^{+0.17}_{-0.19}$	Dre17	8.54 ± 0.14	475.8 ± 8.0	⋯
LHS 3844	b	$0.00623^{+0.00015}_{-0.00015}$	$0.46292792^{+0.0000016}_{-0.0000016}$	(2.25)	$1.32^{+0.02}_{-0.02}$	Van18	69.82 ± 0.74	804.5 ± 8.6	⋯
IL Aqr	b	$0.214^{+0.001}_{-0.001}$	$61.082^{+0.006}_{-0.010}$	$>760.9^{+1.0}_{-1.0}$	(>13.1)	Tri18	0.2823 ± 0.0066	202.9 ± 4.8	Yes
	c	$0.134^{+0.001}_{-0.001}$	$30.126^{+0.011}_{-0.003}$	$>241.5^{+0.7}_{-0.6}$	(>13.7)	Tri18	0.720 ± 0.017	256.4 ± 6.0	Yes

Table 6
(Continued)

Name	Planet	a (au)	P_{orb} (days)	M_p[a] ($M_\oplus$)	R_p[a] ($R_\oplus$)	References[b]	S_{eff} ($S_\odot$)	$T_{eq,p}$ (K)	Potentially HZ
	d	$0.021^{+0.001}_{-0.001}$	$1.938^{+0.001}_{-0.001}$	$>6.910^{+0.220}_{-0.270}$	(>2.54)	Tri18	29.31 ± 0.68	648 ± 15	⋯
	e	$0.345^{+0.001}_{-0.001}$	$124.4^{+0.3}_{-0.7}$	$>15.43^{+1.29}_{-1.27}$	(>3.92)	Tri18	0.1086 ± 0.0025	159.8 ± 3.7	⋯
2MUCD 12171	b	$0.01111^{+0.00034}_{-0.00034}$	$1.51087081^{+0.00000060}_{-0.00000060}$	$0.85^{+0.72}_{-0.72}$	$1.086^{+0.035}_{-0.035}$	Gil17	4.357 ± 0.046	402.1 ± 4.3	⋯
	c	$0.01521^{+0.00047}_{-0.00047}$	$2.4218233^{+0.0000017}_{-0.0000017}$	$1.38^{+0.61}_{-0.61}$	$1.056^{+0.035}_{-0.035}$	Gil17	2.325 ± 0.025	343.7 ± 3.7	⋯
	d	$0.02144^{+0.00066}_{-0.00063}$	$4.049610^{+0.000063}_{-0.000063}$	$0.41^{+0.27}_{-0.27}$	$0.772^{+0.030}_{-0.030}$	Gil17	1.170 ± 0.013	289.5 ± 3.1	Yes
	e	$0.02817^{+0.00083}_{-0.00087}$	$6.099615^{+0.000011}_{-0.000011}$	$0.62^{+0.58}_{-0.58}$	$0.918^{+0.039}_{-0.039}$	Gil17	0.6777 ± 0.0073	252.5 ± 2.7	Yes
	f	$0.0371^{+0.0011}_{-0.0011}$	$9.206690^{+0.000015}_{-0.000015}$	$0.68^{+0.18}_{-0.18}$	$1.045^{+0.038}_{-0.038}$	Gil17	0.3907 ± 0.0042	220.0 ± 2.3	Yes
	g	$0.0451^{+0.0014}_{-0.0014}$	$12.35294^{+0.00012}_{-0.00012}$	$1.34^{+0.88}_{-0.88}$	$1.127^{+0.041}_{-0.041}$	Gil17	0.2644 ± 0.0028	199.6 ± 2.1	Yes
	hr	$0.063^{+0.027}_{-0.013}$	$18.767^{+0.004}_{-0.003}$	(0.39)	$0.752^{+0.032}_{-0.031}$	Gil17, Lug17	0.136 ± 0.030	169 ± 38	

Notes.

[a] The planetary masses and radii shown in parentheses correspond to our adopted mass–radius relation.

[b] Aff16: Affer et al. (2016); Aff19: Affer et al. (2019); Age17: Angelo et al. (2017); Alm15: Almenara et al. (2015); Ang12: Anglada-Escudé et al. (2012); Ang13: Anglada-Escudé et al. (2013); Ang14: Anglada-Escudé et al. (2014); Ang16: Anglada-Escudé et al. (2016); App10: Apps et al. (2010); Ast15: Astudillo-Defru et al. (2015); Ast17a: Astudillo-Defru et al. (2017a); Ast17b: Astudillo-Defru et al. (2017b); Bak18: Bakos et al. (2018); Bay18: Bayliss et al. (2018); Bid14: Biddle et al. (2014); Bon07: Bonfils et al. (2007); Bon11: Bonfils et al. (2011); Bon13b: Bonfils et al. (2013b); Bon17: Bonfils et al. (2018b); Bon18a: Bonfils et al. (2018b); Bon18b: Bonfils et al. (2018a); But17: Butler et al. (2017); Cha09: Charbonneau et al. (2009); Clo17: Cloutier et al. (2017); Dav16: David et al. (2016); Del13: Delfosse et al. (2013); Die18a: (Díez Alonso et al. 2018b); Die18b: (Díez Alonso et al. 2018a); Die19: (Díez Alonso et al. 2019); Dit17: Dittmann et al. (2017); Dre17: Dressing et al. (2017);Fab12: Fabrycky et al. (2012); Fei19: Feinstein et al. (2019); Gil17: Gillon et al. (2017); Gil17: Gillon et al. (2017); Gun19: Günther et al. (2019); Har13: Harpsœet al. (2013); Har15: Hartman et al. (2015); Hir16: Hirano et al. (2016); Hir18: Hirano et al. (2018); Hob18: Hobson et al. (2018); Hob19: Hobson et al. (2019); How10: Howard et al. (2010); Jhu15: Jontof-Hutter et al. (2015); Jon10: Johnson et al. (2010); Jon12: Johnson et al. (2012); Kam18: Kaminski et al. (2018); Liv19: Livingston et al. (2019); LoC13: Lo Curto et al. (2013); Lug17: Luger et al. (2017); Luq18: Luque et al. (2018); Mac14: Maciejewski et al. (2014); Man16a: Mann et al. (2016a); Man16b: Mann et al. (2016b); Men19: Ment et al. (2019); Mon14: Montet et al. (2014); Mor16: Morton et al. (2016); Mui12: Muirhead et al. (2012b); Mui15: Muirhead et al. (2015); Obe16: Obermeier et al. (2016); Per17: Perger et al. (2017); Per19: Perger et al. (2019); Pin18: Pinamonti et al. (2018); Qui14: Quintana et al. (2014); Rei18: Reiners et al. (2018); Rob13: Robertson et al. (2013); Row14: Rowe et al. (2014);Sah16: Sahlmann et al. (2016); San15: Sanchís-Ojeda et al. (2015); Sar18: Sarkis et al. (2018); Sch16: Schlieder et al. (2016); Sin16: Sinukoff et al. (2016); Sou17: Southworth et al. (2017); Smi18: Smith et al. (2018); Sta17: Stassun et al. (2017); Sua17: Suárez Mascareño et al. (2017); Tor15: Torres et al. (2015); Tri18: Trifonov et al. (2018); Tuo14: Tuomi et al. (2014); Van18: Vanderspek et al. (2019); Wel17: Wells et al. (2018); Wit14: Wittenmyer et al. (2014).

[c] Bonfils et al. (2011) gave true mass for LP 905-36 calculated with a Markov chain analysis, $M_p = 8.4^{+4.0}_{-1.5}\ M_\oplus$, but we adopt the minimum mass, $M_2 \sin i$, for consistency.

(This table is available in machine-readable form.)

ORCID iDs

Héctor Martínez-Rodríguez https://orcid.org/0000-0002-1919-228X
José Antonio Caballero https://orcid.org/0000-0002-7349-1387
Carlos Cifuentes https://orcid.org/0000-0003-1715-5087
Anthony L. Piro https://orcid.org/0000-0001-6806-0673

References

Affer, L., Damasso, M., Micela, G., et al. 2019, A&A, 622, A193
Affer, L., Micela, G., Damasso, M., et al. 2016, A&A, 593, A117
Aggarwal, H. R., & Oberbeck, V. R. 1974, ApJ, 191, 577
Agol, E., Jansen, T., Lacy, B., Robinson, T. D., & Meadows, V. 2015, ApJ, 812, 5
Ahn, C. P., Alexandroff, R., Allende Prieto, C., et al. 2012, ApJS, 203, 21
Aksnes, K., & Franklin, F. A. 2001, AJ, 122, 2734
Almenara, J. M., Astudillo-Defru, N., Bonfils, X., et al. 2015, A&A, 581, L7
Angelo, I., Rowe, J. F., Howell, S. B., et al. 2017, AJ, 153, 162
Anglada-Escudé, G., Amado, P. J., Barnes, J., et al. 2016, Natur, 536, 437
Anglada-Escudé, G., Arriagada, P., Tuomi, M., et al. 2014, MNRAS, 443, L89
Anglada-Escudé, G., Boss, A. P., Weinberger, A. J., et al. 2012, ApJ, 746, 37
Anglada-Escudé, G., Tuomi, M., Gerlach, E., et al. 2013, A&A, 556, A126
Apps, K., Clubb, K. I., Fischer, D. A., et al. 2010, PASP, 122, 156
Armstrong, J. C., Barnes, R., Domagal-Goldman, S., et al. 2014, AsBio, 14, 277
Artigau, É., Kouach, D., Donati, J.-F., et al. 2014, Proc. SPIE, 9147, 914715
Astropy Collaboration, Robitaille, T. P., Tollerud, E. J., et al. 2013, A&A, 558, A33
Astudillo-Defru, N., Bonfils, X., Delfosse, X., et al. 2015, A&A, 575, A119
Astudillo-Defru, N., Díaz, R. F., Bonfils, X., et al. 2017a, A&A, 605, L11
Astudillo-Defru, N., Forveille, T., Bonfils, X., et al. 2017b, A&A, 602, A88
Baraffe, I., Homeier, D., Allard, F., & Chabrier, G. 2015, A&A, 577, A42
Barnes, J. W., & O'Brien, D. P. 2002, ApJ, 575, 1087
Barnes, R. 2017, CeMDA, 129, 509
Barnes, R., Deitrick, R., Luger, R., et al. 2016, arXiv:1608.06919
Barnes, R., & Heller, R. 2013, AsBio, 13, 279
Barnes, R., Luger, R., Deitrick, R., et al. 2018, AAS/DPS Meeting, 50, 413.03
Barnes, R., Luger, R., Deitrick, R., et al. 2019, PASP, in press (arXiv:1905.06367.)
Barnes, R., Meadows, V. S., & Evans, N. 2015, ApJ, 814, 91
Barnes, R., Mullins, K., Goldblatt, C., et al. 2013, AsBio, 13, 225
Barnes, R., Raymond, S. N., Jackson, B., & Greenberg, R. 2008, AsBio, 8, 557
Bakos, G. Á, Bayliss, D., Bento, J., et al. 2018, arXiv:1812.09406
Bayliss, D., Gillen, E., Eigmüller, P., et al. 2018, MNRAS, 475, 4467
Bayo, A., Rodrigo, C., Barrado y Navascués, D., et al. 2008, A&A, 492, 277
Benedict, G. F., Henry, T. J., Franz, O. G., et al. 2016, AJ, 152, 141
Ben-Jaffel, L., & Ballester, G. E. 2014, ApJL, 785, L30
Bertout, C. 1989, ARA&A, 27, 351
Berzosa Molina, J., Rossi, L., & Stam, D. M. 2018, A&A, 618, A162
Bianchi, L., Herald, J., Efremova, B., et al. 2011, Ap&SS, 335, 161
Biddle, L. I., Pearson, K. A., Crossfield, I. J. M., et al. 2014, MNRAS, 443, 1810
Bochanski, J. J., Hawley, S. L., Covey, K. R., et al. 2010, AJ, 139, 2679
Bonfils, X., Almenara, J.-M., Cloutier, R., et al. 2018a, A&A, 618, A142
Bonfils, X., Astudillo-Defru, N., Díaz, R., et al. 2018b, A&A, 613, A25
Bonfils, X., Delfosse, X., Udry, S., et al. 2013a, A&A, 549, A109
Bonfils, X., Forveille, T., Delfosse, X., et al. 2005, A&A, 443, L15
Bonfils, X., Gillon, M., Forveille, T., et al. 2011, A&A, 528, A111
Bonfils, X., Gillon, M., Udry, S., et al. 2012, A&A, 546, A27
Bonfils, X., Lo Curto, G., Correia, A. C. M., et al. 2013b, A&A, 556, A110
Bonfils, X., Mayor, M., Delfosse, X., et al. 2007, A&A, 474, 293
Bonnarel, F., Fernique, P., Bienaymé, O., et al. 2000, A&As, 143, 33
Borucki, W. J., Koch, D. G., Basri, G., et al. 2011, ApJ, 728, 117
Bouvier, J. 2013, EAS , 62, 143
Boyajian, T. S., von Braun, K., van Belle, G., et al. 2012, ApJ, 757, 112
Buccino, A. P., Lemarchand, G. A., & Mauas, P. J. D. 2006, Icar, 183, 491
Butler, R. P., Vogt, S. S., Laughlin, G., et al. 2017, AJ, 153, 208
Butler, R. P., Vogt, S. S., Marcy, G. W., et al. 2004, ApJ, 617, 580
Caballero, J. A. 2018, Geosc, 8, 362
Cabrera, J., & Schneider, J. 2007, in ASP Conf. Ser. 366, Transiting Extrasolar Planets Workshop, ed. C. Afonso, D. Weldrake, & T. Henning (San Francisco, CA: ASP), 242
Calvet, N., D'Alessio, P., Hartmann, L., et al. 2002, ApJ, 568, 1008
Campanella, G. 2009, Master's thesis, Sapienza Università di Roma
Chabrier, G. 2003, PASP, 115, 763
Chambers, K. C., Magnier, E. A., Metcalfe, N., et al. 2016, arXiv:1612.05560
Charbonneau, D., Berta, Z. K., Irwin, J., et al. 2009, Natur, 462, 891
Chen, J., & Kipping, D. 2017, ApJ, 834, 17
Clausen, N., & Tilgner, A. 2015, A&A, 584, A60
Cloutier, R., Astudillo-Defru, N., Doyon, R., et al. 2017, A&A, 608, A35
Cnossen, I., Sanz-Forcada, J., Favata, F., et al. 2007, JGRE, 112, E02008
Cutri, R. M., et al. 2012, yCat, 2311, 0
Cutri, R. M., et al. 2014, yCat, 2328, 0
David, T. J., Hillenbrand, L. A., Petigura, E. A., et al. 2016, Natur, 534, 658
Deitrick, R., Barnes, R., Bitz, C., et al. 2018, AJ, 155, 266
Delfosse, X., Bonfils, X., Forveille, T., et al. 2013, A&A, 553, A8
Delfosse, X., Forveille, T., Mayor, M., et al. 1998, A&A, 338, L67
Delfosse, X., Forveille, T., Ségransan, D., et al. 2000, A&A, 364, 217
Dickey, J. O., Marcus, S. L., Hide, R., Eubanks, T. M., & Boggs, D. H. 1994, JGR, 99, 23921
Díez Alonso, E., Caballero, J. A., Montes, D., et al. 2019, A&A, 621, A126
Díez Alonso, E., González Hernández, J. I., Suárez Gómez, S. L., et al. 2018a, MNRAS, 480, L1
Díez Alonso, E., Suárez Gómez, S. L., González Hernández, J. I., et al. 2018b, MNRAS, 476, L50
Dittmann, J. A., Irwin, J. M., Charbonneau, D., et al. 2017, Natur, 544, 333
Dole, S. H. 1964, Habitable Planets for Man (New York: Blaisdell Pub. Co.)
Domingos, R. C., Winter, O. C., & Yokoyama, T. 2006, MNRAS, 373, 1227
Dorn, C., Venturini, J., Khan, A., et al. 2017, A&A, 597, A37
Dressing, C. D., & Charbonneau, D. 2015, ApJ, 807, 45
Dressing, C. D., Vanderburg, A., Schlieder, J. E., et al. 2017, AJ, 154, 207
Driscoll, P. E., & Barnes, R. 2015a, AsBio, 15, 739
Fabrycky, D. C., Ford, E. B., Steffen, J. H., et al. 2012, ApJ, 750, 114
Fassett, C. I., & Minton, D. A. 2013, NatGe, 6, 520
Feinstein, A. D., Schlieder, J. E., Livingston, J. H., et al. 2019, AJ, 157, 40
Forgan, D., & Dobos, V. 2016, MNRAS, 457, 1233
Forgan, D. H. 2017, MNRAS, 470, 416
Fortier, A., Beck, T., Benz, W., et al. 2014, Proc. SPIE, 9143, 91432J
Fortney, J. J., Marley, M. S., & Barnes, J. W. 2007, ApJ, 659, 1661
Forveille, T., Bonfils, X., Lo Curto, G., et al. 2011, A&A, 526, A141
France, K., Arulanantham, N., Fossati, L., et al. 2018, ApJS, 239, 16
Gaia Collaboration, Brown, A. G. A., Vallenari, A., et al. 2018, A&A, 616, A1
Gaia Collaboration, Prusti, T., de Bruijne, J. H. J., et al. 2016, A&A, 595, A1
Gaidos, E., Fischer, D. A., Mann, A. W., & Howard, A. W. 2013, ApJ, 771, 18
Gaidos, E., & Mann, A. W. 2014, ApJ, 791, 54
Gillon, M., Triaud, A. H. M. J., Demory, B.-O., et al. 2017, Natur, 542, 456
Goldreich, P., & Soter, S. 1966, Icar, 5, 375
Gould, A., Bahcall, J. N., & Flynn, C. 1996, ApJ, 465, 759
Green, J. A. M., Huber, M., Waltham, D., Buzan, J., & Wells, M. 2017, E&PSL, 461, 46
Günther, M. N., Pozuelos, F. J., Dittmann, J. A., et al. 2019, NatAs, 3, 1099
Haghighipour, N., Vogt, S. S., Butler, R. P., et al. 2010, ApJ, 715, 271
Han, C., & Han, W. 2002, ApJ, 580, 490
Harpsœ, K. B. W., Hardis, S., Hinse, T. C., et al. 2013, A&A, 549, A10
Hart, M. H. 1978, Icar, 33, 23
Hart, M. H. 1979, Icar, 37, 351
Hartman, J. D., Bayliss, D., Brahm, R., et al. 2015, AJ, 149, 166
Hartmann, L., Calvet, N., Gullbring, E., & D'Alessio, P. 1998, ApJ, 495, 385
Heller, R. 2012, A&A, 545, L8
Heller, R. 2018, Handbook of Exoplanets (Cham: Springer), 35
Heller, R., & Barnes, R. 2013, AsBio, 13, 18
Heller, R., Barnes, R., & Leconte, J. 2011a, OLEB, 41, 539
Heller, R., Leconte, J., & Barnes, R. 2011b, A&A, 528, A27
Heller, R., Rodenbeck, K., & Bruno, G. 2019, A&A, 624, A95
Heller, R., Williams, D., Kipping, D., et al. 2014, AsBio, 14, 798
Henden, A. A., Templeton, M., Terrell, D., et al. 2016, yCat, 2336, 0
Heng, K., & Kopparla, P. 2012, ApJ, 754, 60
Heng, K., Menou, K., & Phillipps, P. J. 2011, MNRAS, 413, 2380
Henning, W. G., O'Connell, R. J., & Sasselov, D. D. 2009, ApJ, 707, 1000
Henry, T. J., Jao, W.-C., Subasavage, J. P., et al. 2006, AJ, 132, 2360
Hernández, J., Hartmann, L., Megeath, T., et al. 2007, ApJ, 662, 1067
Hill, M. L., Kane, S. R., Seperuelo Duarte, E., et al. 2018, ApJ, 860, 67
Hinkel, N. R., & Kane, S. R. 2013, ApJ, 774, 27
Hippke, M., & Angerhausen, D. 2015, ApJ, 810, 29
Hirano, T., Dai, F., Gandolfi, D., et al. 2018, AJ, 155, 127
Hirano, T., Fukui, A., Mann, A. W., et al. 2016, ApJ, 820, 41
Hobson, M. J., Delfosse, X., Astudillo-Defru, N., et al. 2019, A&A, 625, A18
Hobson, M. J., Díaz, R. F., Delfosse, X., et al. 2018, A&A, 618, A103

Høg, E., Fabricius, C., Makarov, V. V., et al. 2000, A&A, 355, L27
Howard, A. W., Johnson, J. A., Marcy, G. W., et al. 2010, ApJ, 721, 1467
Howard, W. S., Tilley, M. A., Corbett, H., et al. 2018, ApJL, 860, L30
Hunter, J. D. 2007, CSE, 9, 90
Ida, S., & Lin, D. N. C. 2004, ApJ, 604, 388
Jackson, B., Barnes, R., & Greenberg, R. 2008a, MNRAS, 391, 237
Jackson, B., Greenberg, R., & Barnes, R. 2008b, ApJ, 678, 1396
Jackson, B., Greenberg, R., & Barnes, R. 2008c, ApJ, 681, 1631
Jeffers, S. V., Schöfer, P., Lamert, A., et al. 2018, A&A, 614, A76
Johns, D., Marti, C., Huff, M., et al. 2018, ApJS, 239, 14
Johnson, J. A., Butler, R. P., Marcy, G. W., et al. 2007, ApJ, 670, 833
Johnson, J. A., Gazak, J. Z., Apps, K., et al. 2012, AJ, 143, 111
Johnson, J. A., Howard, A. W., Marcy, G. W., et al. 2010, PASP, 122, 149
Jontof-Hutter, D., Rowe, J. F., Lissauer, J. J., Fabrycky, D. C., & Ford, E. B. 2015, Natur, 522, 321
Joshi, M. 2003, AsBio, 3, 415
Joshi, M. M., Haberle, R. M., & Reynolds, R. T. 1997, Icar, 129, 450
Kaltenegger, L. 2010, ApJL, 712, L125
Kaminski, A., Trifonov, T., Caballero, J. A., et al. 2018, A&A, 618, A115
Kanodia, S., Wolfgang, A., Stefansson, G. K., Ning, B., & Mahadevan, S. 2019, ApJ, 882, 38
Kasting, J. F., Whitmire, D. P., & Reynolds, R. T. 1993, Icar, 101, 108
Kipping, D. M. 2009, MNRAS, 392, 181
Kipping, D. M., Bakos, G. Á, Buchhave, L., Nesvorný, D., & Schmitt, A. 2012, ApJ, 750, 115
Kipping, D. M., Fossey, S. J., & Campanella, G. 2009, MNRAS, 400, 398
Kipping, D. M., Hartman, J., Buchhave, L. A., et al. 2013, ApJ, 770, 101
Kipping, D. M., Nesvorný, D., Buchhave, L. A., et al. 2014, ApJ, 784, 28
Kipping, D. M., Schmitt, A. R., Huang, X., et al. 2015, ApJ, 813, 14
Kite, E. S., Gaidos, E., & Manga, M. 2011, ApJ, 743, 41
Koll, D. D. B., & Abbot, D. S. 2016, ApJ, 825, 99
Kopparapu, R. K., Ramirez, R., Kasting, J. F., et al. 2013, ApJ, 765, 131
Kopparapu, R. K., Ramirez, R. M., Schottelkotte, J., et al. 2014, ApJL, 787, L29
Kreidberg, L., Luger, R., & Bedell, M. 2019, ApJL, 877, L15
Lainey, V., Arlot, J.-E., Karatekin, Ö, & van Hoolst, T. 2009, Natur, 459, 957
Lambeck, K. 1977, RSPTA, 287, 545
Lambrechts, M., & Johansen, A. 2012, A&A, 544, A32
Lammer, H., Bredehöft, J. H., Coustenis, A., et al. 2009, A&ARv, 17, 181
Lammer, H., Lichtenegger, H. I. M., Kulikov, Y. N., et al. 2007, AsBio, 7, 185
Laskar, J., Joutel, F., & Robutel, P. 1993, Natur, 361, 615
Laskar, J., Robutel, P., Joutel, F., et al. 2004, A&A, 428, 261
Léger, A., Selsis, F., Sotin, C., et al. 2004, Icar, 169, 499
Leggett, S. K., Allard, F., Geballe, T. R., Hauschildt, P. H., & Schweitzer, A. 2001, ApJ, 548, 908
Lin, D. N. C., & Papaloizou, J. 1986, ApJ, 309, 846
Lissauer, J. J., Fabrycky, D. C., Ford, E. B., et al. 2011, Natur, 470, 53
Livingston, J. H., Dai, F., Hirano, T., et al. 2019, MNRAS, 484, 8
Lo Curto, G., Mayor, M., Benz, W., et al. 2013, A&A, 551, A59
Loeb, A., Batista, R. A., & Sloan, D. 2016, JCAP, 8, 040
Lourens, L. J., Wehausen, R., & Brumsack, H. J. 2001, Natur, 409, 1029
Loyd, R. O. P., France, K., Youngblood, A., et al. 2018, ApJ, 867, 71
Luger, R., Sestovic, M., Kruse, E., et al. 2017, NatAs, 1, 129
Luque, R., Nowak, G., Pallé, E., et al. 2018, A&A, 620, A171
Luque, R., Pallé, E., Kossakowski, D., et al. 2019, A&A, 628, A39
Maciejewski, G., Niedzielski, A., Nowak, G., et al. 2014, AcA, 64, 323
Makarov, V. V., & Efroimsky, M. 2014, ApJ, 795, 7
Maldonado, J., Scandariato, G., Stelzer, B., et al. 2017, A&A, 598, A27
Mann, A. W., Dupuy, T., Kraus, A. L., et al. 2019, ApJ, 871, 63
Mann, A. W., Gaidos, E., Mace, G. N., et al. 2016a, ApJ, 818, 46
Mann, A. W., Newton, E. R., Rizzuto, A. C., et al. 2016b, AJ, 152, 61
Marcy, G. W., Butler, R. P., Fischer, D., et al. 2001, ApJ, 556, 296
Marcy, G. W., Butler, R. P., Vogt, S. S., Fischer, D., & Lissauer, J. J. 1998, ApJL, 505, L147
Matsumura, S., Peale, S. J., & Rasio, F. A. 2010, ApJ, 725, 1995
Ment, K., Dittmann, J. A., Astudillo-Defru, N., et al. 2019, AJ, 157, 32
Miller-Ricci, E., Seager, S., & Sasselov, D. 2009, ApJ, 690, 1056
Montet, B. T., Crepp, J. R., Johnson, J. A., Howard, A. W., & Marcy, G. W. 2014, ApJ, 781, 28
Montmerle, T., Augereau, J.-C., Chaussidon, M., et al. 2006, EM&P, 98, 39
Moore, W. B., Schubert, G., Anderson, J. D., & Spencer, J. R. 2007, in Io After Galileo: A New View of Jupiter's Volcanic Moon, ed. R. M. C. Lopes & J. R. Spencer (Berlin: Springer Praxis Books/Geophysical Sciences), 89
Morton, T. D., Bryson, S. T., Coughlin, J. L., et al. 2016, ApJ, 822, 86
Muirhead, P. S., Hamren, K., Schlawin, E., et al. 2012a, ApJL, 750, L37
Muirhead, P. S., Johnson, J. A., Apps, K., et al. 2012b, ApJ, 747, 144
Muirhead, P. S., Mann, A. W., Vanderburg, A., et al. 2015, ApJ, 801, 18
Mullan, D. J., & Bais, H. P. 2018, ApJ, 865, 101
Murray, C. D., & Dermott, S. F. 1999, Solar System Dynamics (Cambridge: Cambridge Univ. Press)
Neron de Surgy, O., & Laskar, J. 1997, A&A, 318, 975
Norman, M. D., & Nemchin, A. A. 2014, E&PSL, 388, 387
Noyola, J. P., Satyal, S., & Musielak, Z. E. 2014, ApJ, 791, 25
Nutzman, P., & Charbonneau, D. 2008, PASP, 120, 317
Obermeier, C., Henning, T., Schlieder, J. E., et al. 2016, AJ, 152, 223
Ochsenbein, F., Bauer, P., & Marcout, J. 2000, A&As, 143, 23
Peale, S. J. 1977a, in IAU Coll. 28, Planetary Satellites, ed. J. A. Burns (Tucson, AZ: Univ. Arizona Press), 87
Peale, S. J. 1977b, AnG, 33, 23
Pepe, F. A., Cristiani, S., Rebolo Lopez, R., et al. 2010, Proc. SPIE, 7735, 77350F
Pepper, J., Gillen, E., Parviainen, H., et al. 2017, AJ, 153, 177
Pérez, F., & Granger, B. E. 2007, CSE, 9, 21
Perger, M., Ribas, I., Damasso, M., et al. 2017, A&A, 608, A63
Perger, M., Scandariato, G., Ribas, I., et al. 2019, A&A, 624, A123
Perryman, M. 2018, The Exoplanet Handbook (Cham: Springer)
Peters, M. A., & Turner, E. L. 2013, ApJ, 769, 98
Pierrehumbert, R., & Gaidos, E. 2011, ApJL, 734, L13
Pinamonti, M., Damasso, M., Marzari, F., et al. 2018, A&A, 617, A104
Piro, A. L. 2018, AJ, 156, 54
Pollack, J. B., Hubickyj, O., Bodenheimer, P., et al. 1996, Icar, 124, 62
Pollack, J. B., Kasting, J. F., Richardson, S. M., & Poliakoff, K. 1987, Icar, 71, 203
Pont, F., Gilliland, R. L., Moutou, C., et al. 2007, A&A, 476, 1347
Price-Whelan, A. M., Sipőcz, B. M., Günther, H. M., et al. 2018, AJ, 156, 123
Quintana, E. V., Barclay, T., Raymond, S. N., et al. 2014, Sci, 344, 277
Quirrenbach, A., Amado, P. J., Caballero, J. A., et al. 2014, Proc. SPIE, 9147, 91471F
Ramírez, R. M. 2018, Geosc, 8, 280
Raymond, S. N., Quinn, T., & Lunine, J. I. 2004, Icar, 168, 1
Reid, I. N., & Gizis, J. E. 1997, AJ, 113, 2246
Reid, I. N., & Hawley, S. L. 2005, New Light on Dark Stars: Red Dwarfs, Low-mass Stars, Brown Dwarfs (Berlin: Springer)
Reiners, A., Ribas, I., Zechmeister, M., et al. 2018, A&A, 609, L5
Renaud, J. P., & Henning, W. G. 2018, ApJ, 857, 98
Reynolds, R. T., McKay, C. P., & Kasting, J. F. 1987, AdSpR, 7, 125
Ribas, I., Tuomi, M., Reiners, A., et al. 2018, Natur, 563, 365
Ricker, G. R., Winn, J. N., Vanderspek, R., et al. 2014, Proc. SPIE, 9143, 914320
Ricker, G. R., Winn, J. N., Vanderspek, R., et al. 2015, JATIS, 1, 014003
Robertson, P., Endl, M., Cochran, W. D., MacQueen, P. J., & Boss, A. P. 2013, ApJ, 774, 147
Rodríguez, R., Schmidt, S. J., Jayasinghe, T., et al. 2018, RNAAS, 2, 8
Rogers, L. A. 2015, ApJ, 801, 41
Rowe, J. F., Bryson, S. T., Marcy, G. W., et al. 2014, ApJ, 784, 45
Sahlmann, J., Lazorenko, P. F., Ségransan, D., et al. 2016, A&A, 595, A77
Sanchís-Ojeda, R., Rappaport, S., Pallè, E., et al. 2015, ApJ, 812, 112
Sarkis, P., Henning, T., Kürster, M., et al. 2018, AJ, 155, 257
Sartoretti, P., & Schneider, J. 1999, A&As, 134, 553
Sasaki, T., & Barnes, J. W. 2014, IJAsB, 13, 324
Sasaki, T., Barnes, J. W., & O'Brien, D. P. 2012, ApJ, 754, 51
Sasaki, T., Stewart, G. R., & Ida, S. 2010, ApJ, 714, 1052
Scalo, J., Kaltenegger, L., Segura, A. G., et al. 2007, AsBio, 7, 85
Schlieder, J. E., Crossfield, I. J. M., Petigura, E. A., et al. 2016, ApJ, 818, 87
Schneider, J., Dedieu, C., Le Sidaner, P., Savalle, R., & Zolotukhin, I. 2011, A&A, 532, A79
Schweitzer, A., Passegger, V. M., Cifuentes, C., et al. 2019, A&A, 625, A68
Seager, S., Kuchner, M., Hier-Majumder, C. A., & Militzer, B. 2007, ApJ, 669, 1279
Segura, A., Kasting, J. F., Meadows, V., et al. 2005, AsBio, 5, 706
Segura, A., Walkowicz, L. M., Meadows, V., Kasting, J., & Hawley, S. 2010, AsBio, 10, 751
Selsis, F., Kasting, J. F., Levrard, B., et al. 2007, A&A, 476, 1373
Selsis, F., Wordsworth, R. D., & Forget, F. 2011, A&A, 532, A1
Shoji, D., & Kurita, K. 2014, ApJ, 789, 3
Showman, A. P., & Kaspi, Y. 2013, ApJ, 776, 85
Showman, A. P., & Polvani, L. M. 2011, ApJ, 738, 71
Simon, A., Szatmáry, K., & Szabó, G. M. 2007, A&A, 470, 727
Simon, A. E., Szabó, G. M., Kiss, L. L., Fortier, A., & Benz, W. 2015, PASP, 127, 1084
Sinukoff, E., Howard, A. W., Petigura, E. A., et al. 2016, ApJ, 827, 78
Skrutskie, M. F., Cutri, R. M., Stiening, R., et al. 2006, AJ, 131, 1163

Smith, A. M. S., Cabrera, J., Csizmadia, S., et al. 2018, MNRAS, 474, 5523
Sotin, C., Grasset, O., & Mocquet, A. 2007, Icar, 191, 337
Southworth, J., Mancini, L., Madhusudhan, N., et al. 2017, AJ, 153, 191
Stassun, K. G., Collins, K. A., & Gaudi, B. S. 2017, AJ, 153, 136
Stephenson, C. B. 1986, AJ, 91, 144
Suárez Mascareño, A., González Hernández, J. I., Rebolo, R., et al. 2017, A&A, 605, A92
Sullivan, P. W., Winn, J. N., Berta-Thompson, Z. K., et al. 2015, ApJ, 809, 77
Szabó, G. M., Szatmáry, K., Divéki, Z., & Simon, A. 2006, A&A, 450, 395
Szabó, R., Szabó, G. M., Dálya, G., et al. 2013, A&A, 553, A17
Tarter, J. C., Backus, P. R., Mancinelli, R. L., et al. 2007, AsBio, 7, 30
Teachey, A., & Kipping, D. M. 2018, SciA, 4, eaav1784
Teachey, A., Kipping, D. M., & Schmitt, A. R. 2018, AJ, 155, 36
Tonry, J. L., Stubbs, C. W., Lykke, K. R., et al. 2012, ApJ, 750, 99
Torres, G., Kipping, D. M., Fressin, F., et al. 2015, ApJ, 800, 99
Trifonov, T., Kürster, M., Zechmeister, M., et al. 2018, A&A, 609, A117
Tuomi, M., Jones, H. R. A., Barnes, J. R., Anglada-Escudé, G., & Jenkins, J. S. 2014, MNRAS, 441, 1545
Tuomi, M., Jones, H. R. A., Jenkins, J. S., et al. 2013, A&A, 551, A79
Turbet, M., Leconte, J., Selsis, F., et al. 2016, A&A, 596, A112
Tyler, R. H., Henning, W. G., & Hamilton, C. W. 2015, ApJS, 218, 22
Udry, S., Bonfils, X., Delfosse, X., et al. 2007, A&A, 469, L43
Underwood, D. R., Jones, B. W., & Sleep, P. N. 2003, IJAsB, 2, 289
Upgren, A. R., Grossenbacher, R., Penhallow, W. S., MacConnell, D. J., & Frye, R. L. 1972, AJ, 77, 486
Van Der Walt, S., Colbert, S. C., & Varoquaux, G. 2011, CSE, 13, 22
van Leeuwen, F. 2007, A&A, 474, 653
Vanderburg, A., Rappaport, S. A., & Mayo, A. W. 2018, AJ, 156, 184
Vanderspek, R., Huang, C. X., Vanderburg, A., et al. 2019, ApJL, 871, L24
Veeder, G. J., Davies, A. G., Matson, D. L., et al. 2012, Icar, 219, 701
Vidotto, A. A., Jardine, M., Morin, J., et al. 2013, A&A, 557, A67
Virtanen, P., Gommers, R., Oliphant, E., et al. 2019, arXiv:1907.10121
Vogt, S. S., Butler, R. P., & Haghighipour, N. 2012, AN, 333, 561
Vogt, S. S., Butler, R. P., Rivera, E. J., et al. 2010, ApJ, 723, 954
Way, M. J., Del Genio, A. D., Aleinov, I., et al. 2018, ApJS, 239, 24
Weiss, L. M., & Marcy, G. W. 2014, ApJL, 783, L6
Wells, R., Poppenhaeger, K., & Watson, C. A. 2018, MNRAS, 473, L131
Williams, J. G. 1994, AJ, 108, 711
Williams, J. G., Sinclair, W. S., & Yoder, C. F. 1978, GeoRL, 5, 943
Wittenmyer, R. A., Tuomi, M., Butler, R. P., et al. 2014, ApJ, 791, 114
Wolfgang, A., Rogers, L. A., & Ford, E. B. 2016, ApJ, 825, 19
Wordsworth, R. 2015, ApJ, 806, 180
Wu, Y., & Lithwick, Y. 2013, ApJ, 772, 74
Wunderlich, F., Godolt, M., Grenfell, J. L., et al. 2019, A&A, 624, A49
Yang, J., Cowan, N. B., & Abbot, D. S. 2013, ApJL, 771, L45
Yang, J., Liu, Y., Hu, Y., & Abbot, D. S. 2014, ApJL, 796, L22
Yoder, C. F. 1979, Natur, 279, 767
Yoder, C. F. 1995, in Global Earth Physics: A Handbook of Physical Constants, ed. T. J. Ahrens (Washington, DC: AGU), 1
Zacharias, N., Finch, C. T., Girard, T. M., et al. 2013, AJ, 145, 44
Zechmeister, M., Dreizler, S., Ribas, I., et al. 2019, A&A, 627, A49
Zechmeister, M., Kürster, M., & Endl, M. 2009, A&A, 505, 859
Zhang, K., & Hamilton, D. P. 2006, AAS/DPS Meeting, 38, 01.07
Zhuang, Q., Gao, X., & Yu, Q. 2012, ApJ, 758, 111
Zollinger, R. R., Armstrong, J. C., & Heller, R. 2017, MNRAS, 472, 8
Zsom, A., Seager, S., de Wit, J., & Stamenković, V. 2013, ApJ, 778, 109